RDECOM TR 10-D-106

**U.S. ARMY RESEARCH,
DEVELOPMENT AND
ENGINEERING COMMAND**

TITLE: Comparisons of Theoretical Methods for Predicting Airfoil Aerodynamic Characteristics

AUTHOR: Mark D. Maughmer and James G. Coder

COMPANY NAME: Airfoils, Incorporated

COMPANY ADDRESS: 122 Rose Drive
Port Matilda PA 16870-7535

DATE (MONTH YEAR): August 2010

FINAL REPORT: Contract Number W911W6-07-C-0047, SBIR Phase II, Topic No. A06-006, Proposal No. A2-2972

Prepared for:

**U.S. ARMY RESEARCH, DEVELOPMENT AND ENGINEERING COMMAND,
AVIATION APPLIED TECHNOLOGY DIRECTORATE, FORT EUSTIS, VA 23604-5577**

Comparisons of Theoretical Methods for Predicting Airfoil Aerodynamic Characteristics

Mark D. Maughmer and James G. Coder
The Pennsylvania State University
University Park, Pennsylvania 16802

Airfoils, Incorporated Subcontract
Final Report
August 2010

Comparisons of Theoretical Methods for Predicting Airfoil Aerodynamic Characteristics

Mark D. Maughmer and James G. Coder
The Pennsylvania State University
University Park, Pennsylvania 16802

Airfoils, Incorporated Subcontract
Final Report
August 2010

Abstract

A number of airfoils intended for VTOL/Rotorcraft applications were tested in the Penn State Low-Speed, Low-Turbulence Wind Tunnel, and the results of these tests compared with those predicted using several well-known theoretical methods. The airfoils considered are the E 387 and the S406, S407, S411, S414, and the S415, and the theoretical methods used are the potential-flow/integral boundary-layer methods, PROFIL07 and XFOIL 6.94, the Euler solver/integral boundary-layer method, MSES 3.05, and the Reynolds-averaged Navier-Stokes solver, OVERFLOW 2.1ae. In addition, several cases were considered using the Navier-Stokes solver, FLUENT 12.1.2, which incorporates the Langtry-Menter four-equation turbulence model that has demonstrated some capability of capturing the transition process. While none of the methods considered was consistently the best overall, the drag predictions of the codes incorporating boundary-layer methods generally agreed better with the experimental results than did those of the Navier-Stokes solvers. All of the theoretical methods frequently over-predicted the maximum lift coefficient, although an empirical criterion developed for use with PROFIL yielded reasonably close agreement with the measurements. The Langtry-Menter turbulence model employed in FLUENT 12.1.2 shows promise in being able to model the transition process, including the development of laminar separation bubbles.

Nomenclature

c	=	airfoil chord
c_d	=	profile-drag coefficient
c_l	=	section lift coefficient
c_m	=	section pitching-moment coefficient about the quarter-chord point
C_P	=	pressure coefficient, $(p_l - p_\infty)/q_\infty$
L.	=	lower surface
p	=	pressure
q	=	dynamic pressure
R	=	Reynolds number based on free-stream conditions and airfoil chord
S.	=	boundary-layer separation location, x_S/c
T.	=	boundary-layer transition location, x_T/c
U.	=	upper surface
y^+	=	non-dimensional turbulent boundary layer coordinate

Subscripts

l	local point on airfoil
max	maximum
S	separation
T	transition
∞	free-stream conditions

Introduction

Over the past several years, a number of airfoils intended for VTOL/Rotorcraft applications have been tested in the Penn State Low-Speed, Low-Turbulence Wind Tunnel. These airfoils are targeted for a variety of applications and, therefore, cover a

broad range of geometries and operating conditions. The thickness ratios of the airfoils tested range from 0.09 to 0.18 and the Reynolds numbers from 60,000 to 2,000,000.

One of the goals of these tests is to provide a consistent set of experimental data with which to compare several theoretical methods currently in use for predicting airfoil aerodynamic characteristics. The airfoils used for this comparison are the S406, S407, S411, S414, and the S415. The specifications and details of the design and testing of these airfoils are presented in Refs. [1-5]. In addition to these airfoils, the E 387 was also tested as a part of qualifying the Penn State wind tunnel for this work [6]. The experimental measurements made on these airfoils are compared with the predictions of PROFIL07 [7], OVERFLOW 2.1ae [8,9], XFOIL 6.94 [10], and MSES 3.05 [11]. Finally, a few comparisons are made with results from FLUENT 12.1.2 [12].

Although wind-tunnel measurements were made with free transition, fixed transition, and scaled NACA standard roughness, only comparisons with free transition will be presented and only at the lowest and highest Reynolds numbers at which a particular airfoil was tested. It should be noted that comparisons of measured pressure distributions with those predicted by PROFIL and MSES are included in Refs. [1-6].

Wind-Tunnel Experiments

Wind Tunnel, Model, and Data-Acquisition System

The Penn State University Low-Speed, Low-Turbulence Wind Tunnel is a closed-throat, single-return atmospheric facility. The test section is rectangular and is 101.3 cm (39.9 in) high and 147.6 cm (58.1 in) wide with filleted corners. The maximum test-section speed is 67 m/s (220 ft/s). Airfoil models are mounted vertically in the test section and attached to computer-controlled turntables that allow the angle of attack to be set. The turntables are flush with the floor and ceiling and rotate with the model. The axis of rotation is between the quarter- and half- chord locations on the model. The gaps between the model and the turntables are sealed to prevent leaks.

The flow quality of the Penn State wind tunnel has been measured and documented [13]. At a velocity of 46 m/s (150 ft/s), the flow angularity is everywhere below ±0.25 deg. in the test section. At this velocity, the mean velocity variation in the test section is below ±0.2 percent, and the turbulence intensity is less than 0.045 percent.

The models used in these experiments range in chords from 15.2 cm (6.0 in) to 53.3 cm (21.0 in). They were mounted vertically in the wind tunnel and completely spanned the height of the test section. The models were produced from solid aluminum using a numerically-controlled milling machine. Each model has approximately 33 pressure orifices on the upper surface and roughly the same number on the lower surface. Each orifice has a diameter of 0.51 mm (0.020 in) and is drilled perpendicular to the surface. The orifice locations are staggered in the spanwise direction to minimize the influence of an orifice on those downstream. Additional details regarding the models and their fabrication are contained in Refs. [1-6].

To obtain drag measurements, a wake-traversing, Pitot-static pressure probe is mounted from the ceiling of the tunnel. A traversing mechanism incrementally positions the probe across the wake, which automatically aligns with the local wake-centerline streamline as the angle of attack changes.

The basic wind-tunnel pressures are measured using pressure-sensing diaphragm transducers. Measurements of the pressures on the model are made by an automatic pressure-scanning system. Data are obtained and recorded with an electronic data-acquisition system.

Experimental Methods

The surface pressures measured on the model are reduced to standard pressure coefficients and numerically integrated to obtain section normal- and chord-force coefficients, as well as section pitching-moment coefficients about the quarter-chord point. Section profile-drag coefficients are computed from the wake total and static pressures using standard procedures [14]. At most post-stall angles of attack, however, wake surveys are not performed and profile drag coefficients are computed from normal- and chord-force coefficients as obtained from pressure integration. Low-speed wind-tunnel boundary corrections are applied to the data [15]. A total-pressure-tube displacement correction, although quite small, is also applied to the wake-survey probe [14].

As is clear from the procedures prescribed in Ref. [16], the uncertainty of a measured force or moment coefficient depends on the operating conditions and generally

increases with increasing angles of attack. In the higher lift regions, for which the uncertainty is the greatest, the measured lift coefficients have an uncertainty of Δc_l = ±0.005. The uncertainty of drag coefficients measured in the low-drag range is Δc_d = ±0.00005 while, as the angle of attack approaches stall, this increases to Δc_d = ±0.00015. The pitching-moment coefficients have an uncertainty of Δc_m = ±0.002

In addition to making the quantitative measurements indicated, flow-visualization studies were performed using fluorescent oil [17]. These methods were used not only to determine transition locations and regions of separated flow as they depend on angle of attack, but also to verify the two-dimensionality of the tests. As is typically the case in this facility, it was found in all cases that the flow over the model was two-dimensional up to and slightly beyond the angle of attack at which the maximum lift coefficient occurs.

Facility Qualification

While the attainment of high flow quality is certainly a requisite for making meaningful airfoil aerodynamic measurements, additional confidence in the Penn State facility is gained by making comparisons with data taken elsewhere. For this purpose, the Low-Turbulence Pressure Tunnel (LTPT) at the NASA Langley Research Center [18] and the Low-Speed Wind Tunnel at Delft University of Technology in The Netherlands [19] are perhaps the two most highly regarded two-dimensional, low-speed wind tunnels. For low Reynolds number airfoil aerodynamics, a benchmark data set is that obtained with the E 387 airfoil in LTPT [20]. In Fig. 1, these results are compared with those from the Penn State tunnel for Reynolds numbers ranging from $R = 0.6 \times 10^5$ to 4.6×10^5 [6]. For additional comparison, available results from Delft [21] and Stuttgart [22] are included. Except for post-stall aerodynamics, which are highly three-dimensional and not all that meaningful with respect to two-dimensional measurements, the agreement of the data from the Penn State facility with that of LTPT is excellent. The quality of this agreement is emphasized by the increasing deviation of the Delft and Stuttgart results from those of LTPT and Penn State as the Reynolds number decreases. In addition to the force and moment data comparisons presented here, pressure distributions and transition

locations measured at Penn State also show excellent agreement with those obtained in the Langley facility [6].

In Fig. 2, Penn State tunnel measurements made on the laminar-flow S805 wind turbine airfoil [23] are compared with those obtained using the same wind-tunnel model at Delft [24]. These data, with Reynolds numbers ranging from $R = 0.5 \times 10^6$ to 1.5×10^6, also demonstrate excellent agreement. Although not presented here, pressure distributions and measured transition locations obtained at Penn State also show excellent agreement with those of the Delft experiments [23].

Tests Performed

Each model was tested through a range of Reynolds numbers with transition free (smooth) and with transition fixed by grit roughness near the leading edge or, for the lower Reynolds numbers tested, by properly-sized zig-zag turbulator tape. Both the grit roughness and the turbulator tape were employed to simulate full-chord turbulent flow. The grit roughness was sized to the critical roughness height using the method of Ref. [25] and sparsely distributed in spanwise strips near the leading edge. The tape was sized using a stethoscope to determine the minimum height required to cause transition. All except the E 387 and the S407 airfoils were also tested with a roughness equivalent to NACA standard roughness [26], which consists of sparsely-distributed grit applied around the leading edges of the models.

The equivalent free-stream Mach number did not exceed 0.2 for any of the tests conducted.

Methods of Theoretical Prediction Employed

PROFIL07

PROFIL [7], commonly known as the Eppler code, consists of an inverse conformal mapping method for design and a panel method coupled with an integral boundary-layer calculation for analysis. Although it is able to analyze cascades, it is primarily intended for single-element airfoils. Boundary-layer displacement-thickness iteration is an option, but as it increases the computational overhead and only influences the value of the zero-lift angle of attack, it is not usually employed. The boundary-layer

method predicts transition using a full e^N method. In this implementation, over 40,000 solutions to the Orr-Sommerfeld equation are tabulated from which the amplification rates of the Tollmien-Schlichting waves can be interpolated. The amplification rates depend on the displacement-thickness Reynolds number, the displacement-to-momentum thickness shape factor, and a non-dimensional frequency, all of which are determined as the boundary-layer development is calculated. The frequency of the first unstable Tollmien-Schlichting wave is determined, and a range of frequencies around it is defined. The amplification of each of these frequencies is evaluated. At every position along the airfoil surface, the maximum amplification is found, and transition is assumed when the natural logarithm of the amplification rate for any of the frequencies reaches a critical value, N. For the predictions presented here, the value of N was set to 11.

It should be noted that unlike the other theoretical methods employed here, for which the lift coefficients are obtained by integrating the pressure distributions, the lift coefficients from PROFIL are calculated from the lift-curve slope and the angle of attack relative to the zero-lift line. Because the value of the maximum lift coefficient computed by this method is not always realistic, an empirical criterion has been applied to the computed results. This criterion assumes that the maximum lift coefficient is achieved when the upper-surface drag coefficient contribution reaches a certain value, which depends on the value of the Reynolds number.

Although the outer flow solution is obtained using potential flow, the program employs a Mach number correction valid for locally subsonic flows. This correction gives reasonable results up to the critical Mach number. The analysis capability of this program is very fast and robust compared to other predictive tools.

XFOIL 6.94

XFOIL [10] also makes use of a potential flow solution that is coupled with an integral boundary layer. It is also applicable only to single-element airfoils. Iteration between the outer and inner flow solutions is continued until a suitable convergence on the boundary-layer displacement thickness is achieved. In this way, reasonably accurate viscous pressure distributions, which capture the influence of limited trailing-edge separation and laminar separation bubbles, are predicted. XFOIL makes use of an

approximate e^N-envelope method to calculate transition [27]. Here, rather than tracking the amplification rates corresponding to all frequencies (or a range of frequencies as is the case with PROFIL), this method tracks only the most amplified frequency at a given point on the airfoil downstream from the point of instability to obtain the amplitude of that disturbance. Transition is assumed when this integrated amplitude reaches an empirically determined value. The amplitude curves used here are straight-line approximations to the actual envelopes determined using Falkner-Skan boundary-layer profiles. The simplifications used here are most called into question in cases where the shape factor varies rapidly.

XFOIL is only slightly less robust than PROFIL, in that convergence is occasionally problematic. Like PROFIL, it also makes use of a correction for Mach number that allows for reasonable predictions up to the critical Mach number.

MSES 3.05

MSES [11] employs an Euler solver for the outer flow and an integral boundary layer, similar to that of XFOIL, for the viscous layer. As an Euler method, it is able to predict the aerodynamic characteristics of airfoils in the transonic region. Unlike PROFIL and XFOIL, it can also handle multi-element airfoils.

MSES can predict transition using a full e^N method, in which a Newton iteration method is used to find the critical Tollmien-Schlichting frequency [28], or by means of the approximate envelope e^N method like that used in XFOIL [27]. The predictions presented here used the full e^N method, whereas those obtained using the envelope e^N method are compared with PROFIL and wind-tunnel results in Refs. [1-6].

As expected, the increased capabilities of MSES result in it not being as easy to use or as robust as PROFIL and XFOIL. In particular, the program requires considerably more run time and convergence can be problematic.

OVERFLOW 2.1ae

OVERFLOW [9] is a three-dimensional Reynolds-averaged Navier-Stokes (RANS) solver that uses structured overset grids. It can do two-dimensional calculations using a variety of one- and two-equation turbulence models. The Spalart-Allmaras one-

equation turbulence model with streamline curvature corrections was used to obtain the solutions presented, which were run with a non-time-accurate scheme until convergence of the flow field residuals was achieved.

Unlike PROFIL, XFOIL, and MSES, there is no treatment of natural transition in OVERFLOW. It is possible to specify so-called "trip-lines" in the flowfield, but for the present calculations the flowfield is treated as being fully turbulent. It is important to make a distinction from that of running a Navier-Stokes solver "fully turbulent" to that of having a "fully turbulent" boundary layer. In the former case, it means that the production terms of the turbulence model are always active. As there is no transition modeling, however, this means that the viscous layer from the leading edge is "laminar-like," and gradually becomes more "turbulent-like" downstream. Thus, the sudden change from a laminar to a turbulent boundary layer observed in nature is not captured. For this reason, rather than the distinct contributions of a given amount of laminar and turbulent boundary-layer being taken into account, the predicted profile-drag coefficient is essentially the result of the viscous development being averaged over its length.

All overset grids were generated with Chimera Grid Tools 2.0 [29], producing O-type body-fitted grids and Cartesian far-field grids. Best practices in overset grid generation were followed throughout the gridding process [30].

ANSYS FLUENT 12.1.2

FLUENT [12] is an unstructured Navier-Stokes solver that can operate in either two-dimensional or three-dimensional modes. For the cases examined here, it was employed as a two-dimensional, RANS solver. The user is allowed a wide selection of turbulence models and here, the four-equation transition SST turbulent model was used. The solution schemes were initialized using non-time-accurate marching and then switched to implicit time-accurate marching until force convergence was achieved.

The additional transport equations of the turbulence model allow for the prediction of transition using the local variables of the flowfield [31]. Both natural transition and transition via a laminar separation bubble can be predicted using this model.

All grids used for the FLUENT calculations were generated with GAMBIT 2.4.6 [32]. The grids were generated such that the y^+ value of the first boundary-layer point is less than 1.0 in the turbulent regions.

Comparisons of Experimental and Theoretical Results

E 387

The E 387 airfoil was designed by Richard Eppler in the mid-1960s for use on model sailplanes. Because it was designed specifically for the appropriate lift coefficients and Reynolds numbers required by its application, it (along with other Eppler designs) provided a significant improvement over other airfoils available at that time. With the interest in small, uninhabited flight vehicles that percolated in the early 1980s, this airfoil became a touchstone for much of the research directed at increasing the understanding of low Reynolds number airfoil aerodynamics. As already mentioned, the data obtained on this airfoil in LTPT at that time are still regarded as the standard against which other low Reynolds number experiments are compared [20]. The same test matrix that had been run at LTPT was run at Penn State, including the Reynolds number range of 60,000 to 460,000. In addition to measurements taken on the clean model, data were also obtained for transition fixed at 5-percent chord on both the upper and lower surfaces. Full details of these experiments are presented in Ref. [6].

The aerodynamic characteristics predicted for R = 300,000 by PROFIL and OVERFLOW are compared to the Penn State wind-tunnel measurements in Fig. 3(a), while those of XFOIL and MSES are presented along with those measured at Penn State in Fig. 3(b). As can be observed in Fig. 3(a), PROFIL predicts the corners of the low-drag region, although they are shifted down to slightly lower lift coefficients. The upper corner of the low-drag region is a consequence of the forward movement of the transition point on the upper surface with increasing lift coefficients, and the lower corner a consequence of the forward movement of the transition point on the lower surface with decreasing lift coefficients. The predicted drag coefficients are within ten counts of the measured results. Because the turbulence model in OVERFLOW is unable to predict transition, it does not replicate the sharp corners on the drag polar. The value of $c_{l,max}$ is predicted quite well by both PROFIL and OVERFLOW, as are the pitching-moment coefficients. In fact, the

moment coefficients are predicted very well by OVERFLOW in the linear range of the lift curve.

Figure 3(b) presents the predicted results of XFOIL, MSES along with the measured Penn State data. The two predicted drag results are very similar to one another and, like PROFIL, within about 10 counts of those measured. The value of $c_{l,max}$ is slightly over-predicted by XFOIL and slightly under-predicted by MSES. The pitching-moment coefficients are well predicted in the linear range for both methods, although MSES predictions are slightly better than those of XFOIL at the higher angles of attack.

S406

The S406 airfoil was designed for the working section of the rotor of a relatively small helicopter [1]. It has a thickness ratio of 0.1425 and was designed to have reasonably high lift, low profile drag, and docile stall characteristics. Given the operational Reynolds number range and the anticipated manufacturing methods, the attainment of laminar flow was thought to be worth considering. The design was constrained to not have a pitching-moment coefficient any more negative than -0.05, although the wind-tunnel measurements show that this requirement was not achieved.

The measured aerodynamic characteristics for R = 500,000 are compared to those theoretically predicted in Fig. 4, while those for R = 1,500,000 are compared in Fig. 5. In all cases, the values of $c_{l,max}$ are over-predicted by the theoretical methods. The empirically-based prediction used with PROFIL is the closest, being about 6.5 percent too high, while that of OVERFLOW is nearly 23 percent too high. The predictions of profile drag are also fairly varied. For this airfoil, XFOIL is the most successful at predicting the drag coefficients, followed closely by the predictions of MSES. The profile drag predictions of PROFIL are roughly 10 counts too high, while those of OVERFLOW about 20 counts too high.

Finally, the predicted pitching-moment coefficients also vary a great deal between the different methods, with XFOIL and MSES being the best. At the higher Reynolds number, shown in Fig. 5, the evaluation of the pitching-moment coefficient predictions is about the same as it was for the lower Reynolds number, while those of $c_{l,max}$ and c_d are very different, with PROFIL providing the best predictions and OVERFLOW the worst.

S407

The S407 airfoil, designed to operate on the tandem rotors of a high altitude UAV, has a thickness ratio of 0.1143 [2]. For its intended operating environment and conditions, designing this airfoil for extended regions of laminar flow warranted consideration. Its design requirements also include the achievement of high maximum lift and low profile drag. While the specified pitching-moment coefficient constraint was satisfied, the desire for docile stall characteristics was not.

In Fig. 6, the wind-tunnel measurements for R = 70,000 are compared with those predicted by the theoretical methods. At the lower end of the Reynolds number range for this airfoil, the aerodynamics are largely characterized by the growth and disappearance of laminar separation bubbles, and consequently, the measurements and the predictions are both difficult. Nevertheless, all of the theoretical methods except OVERFLOW match the qualitative behavior of the experimental drag polar and the value of $c_{l,max}$ remarkably well, while the actual values of the profile-drag coefficients predicted by PROFIL and XFOIL are reasonably close to those measured. The value of the pitching-moment coefficient as it depends on angle of attack is well predicted by both XFOIL and MSES.

The comparisons of experimental and predicted results are repeated for R = 600,000 in Fig. 7. At this Reynolds number, with the exception of $c_{l,max}$, all of the theoretical predictions are closer to those measured than they were at the lower Reynolds number. The profile-drag coefficients and the value of $c_{l,max}$ predicted by PROFIL are the closest to the wind-tunnel results. XFOIL and MSES under-predict the profile-drag coefficients values by roughly 10 to 20 counts over the minimum drag region of the polar, and over-predict $c_{l,max}$ by about 10 percent. OVERFLOW over-predicts the minimum drag coefficient by nearly 30 counts and $c_{l,max}$ by about 10 percent. XFOIL and MSES provide the best prediction of the pitching-moment coefficient with angle of attack, although PROFIL and OVERFLOW produce reasonable predictions.

S411

The S411 airfoil is designed to specifications very similar to those of the S406, the primary difference being that the S411 airfoil is required to have a tab at trailing edge that is 5-percent chord [3]. In this case, the tab is not used for “zeroing out” the pitching-

moment coefficient at zero deflection, but rather as a tracking tab on the rotor blade. The thickness ratio of the S411 airfoil is 0.1400.

The aerodynamic characteristics for R = 500,000 as predicted by the theoretical methods employed here are compared in Fig. 8 with those obtained experimentally. The lack of a well-defined upper-limit of the low-drag range allows the drag polar predicted by OVERFLOW to better follow the general shape of the polar than would otherwise be the case. Unlike the other theoretical methods, it does not predict the rapid changes in drag at the lower limit of the low-drag range that is caused by the movement of both the lower-surface separation and transition locations with angle of attack. It does, however, predict the rapid increase in drag at negative lift coefficients that is caused by increasing flow separation on the lower surface.

The drag predictions of MSES in the low-drag region are excellent, while the other methods over-predict the drag in the middle of the polar. MSES and XFOIL over-predict $c_{l,max}$ by nearly 15 percent and OVERFLOW by nearly 20 percent. The empirical criterion used with PROFIL again provides the best estimate of $c_{l,max}$. The XFOIL prediction of the pitching-moment coefficient as it depends on the angle of attack is excellent, although the other theoretical methods also provide reasonable results.

These comparisons are repeated for R = 1,500,000 in Fig. 9. For this Reynolds number, the drag predictions in the low-drag region of PROFIL and XFOIL are considerably better than those of the preceding case. The drag predictions of MSES are slightly worse, while those of OVERFLOW are now up to 35 counts too high and convergence at lower lift coefficients was not achieved. Except for the value predicted using the empirical criteria with PROFIL, all of the predicted $c_{l,max}$ values are over 25 percent greater than the experimental result. XFOIL and MSES both provide a reasonably good prediction of the pitching-moment coefficient as it depends on the angle of attack, although PROFIL and OVERFLOW predictions are also acceptable.

S414

The S414 explores the concept of a slotted, natural-laminar-flow (SNLF) airfoil [4]. It is designed to roughly the same specifications as the S406 and S411 airfoils,

although it achieves significantly higher lift and lower drag. It has a thickness ratio of 0.1422.

Because it is a two-element airfoil, only OVERFLOW and MSES are able to predict its aerodynamic characteristics. The predicted characteristics for R = 700,000 that are generated by these two methods are compared with those obtained experimentally in Fig. 10, while similar comparisons for R = 1,500,000 are presented in Fig. 11. For both Reynolds numbers, the drag polar predictions of MSES are very good while, as expected, the upper and lower limits of the low-drag region cannot be captured by OVERFLOW. In addition, OVERFLOW over-predicts the drag coefficients in the low-drag region by as much as 80 counts. The pitching-moment coefficient predictions of both methods at both Reynolds numbers are reasonable. MSES over-predicts $c_{l,max}$ for both Reynolds numbers by about 9 percent, while OVERFLOW under-predicts $c_{l,max}$ at R = 700,000 by 7 percent, and at R = 1,500,000 by nearly 14 percent.

From the measurements, although it has a very hard stall, it is notable that for R = 700,000 the S414 airfoil achieves a value of $c_{l,max}$ of about 1.72 and a minimum drag coefficient of about 80 counts. At R = 1,500,000, $c_{l,max}$ is nearly 2.0 and the drag coefficient is less than 60 counts.

S415

The S415 is part of an effort exploring the use of a morphing rotor airfoil [5]. The S415 is designed to be the airfoil used during hover, while for forward flight it would morph into the S418 airfoil [33], which is better suited for those conditions. The S415 airfoil has a thickness ratio of 0.1412.

For R = 1,000,000, the predicted aerodynamic characteristics are shown with measured results in Fig. 12. It can be observed that the PROFIL drag-coefficient predictions are in excellent agreement with the wind-tunnel results. The profile-drag predictions of OVERFLOW are roughly 50 counts too large, and it is unable to predict the upper- and lower-limits of the low-drag region. The drag coefficient values in the middle of the drag polar as predicted by XFOIL and MSES are just a few counts too low. The empirical criterion used with PROFIL provides a reasonably accurate estimation of $c_{l,max}$, while the OVERFLOW prediction is about 19 percent too large. XFOIL and MSES

both predict $c_{l,max}$ to be about 8 percent too large, along with the critical angle of attack being predicted about 3 degrees high. All of the methods used predict the pitching-moment coefficient reasonably well, although PROFIL over-predicts the magnitude of the nose-down pitching-moment coefficient by about 0.02.

These comparisons are repeated for R = 2,000,000 in Fig. 13.

Discussion of Results

From the comparisons of the results generated by the different theoretical methods with the wind-tunnel measurements, it is clear that those incorporating boundary-layer methods provide a more reliable drag prediction than does OVERFLOW. Generally, the drag coefficients and the corners of the low-drag region are well predicted by these methods. As a consequence of the fact that the transition process is not being modeled or accounted for, the Navier-Stokes solver, making use of the available turbulence models, is much less effective. At the Reynolds numbers being considered for these results, transition can be due to Tollmien-Schlichting instabilities, or more likely, by means of laminar separation bubbles. In either case, transition is a very well demarked process in the development of the flow over a surface. As such, each event in the process occurs relatively quickly and over a small extent of the chord. The turbulence models generally used in the CFD predictions, on the other hand, produce a development in which the inherent turbulence grows slowly from "laminar-like" behavior of the viscous layer to one that is more and more "turbulent-like." Thus, the actual "burst" of transition is not captured and, consequently, there is no chance of reliably predicting the proper contributions of the laminar boundary layer and the turbulent boundary layer to the total profile drag of an airfoil [34]. For airfoils designed to have a well defined low-drag region, it is not possible for these turbulence models to predict the sharp corners that define the limits of such regions.

In looking at the maximum lift coefficient predictions of the theoretical methods considered, it is interesting that the most reliable is obtained with the simple empirical criterion based on the upper-surface profile drag contribution that is used with PROFIL. In the worst case, this method over-predicted $c_{l,max}$ by approximately 9 percent, while more typically the predicted value was within 3 percent of the measured one.

The predictions of XFOIL and MSES are comparable, albeit both often over-predict the value of the maximum lift coefficient. The worst over-prediction of $c_{l,max}$ by XFOIL was by about 15 percent, while the average predicted value was within 11 percent of the measured one. MSES over-predicted $c_{l,max}$ by as much as 20 percent, although the average error was comparable to XFOIL at just less than 11 percent.

Overall, it is found that the codes incorporating integral boundary-layer methods predict $c_{l,max}$ reasonably well when a relatively steep adverse pressure gradient exists on the upper surface such that there is a very rapid forward movement of the separation point with increasing angles of attack. When the pressure gradient is less steep, the forward movement of the separation point is much more gradual and these methods consistently over-predict the value of $c_{l,max}$.

OVERFLOW over-predicted $c_{l,max}$ by as much as 26 percent, while more typically, the value was within 18 percent of that measured. One explanation for the large errors with the CFD predictions of $c_{l,max}$ could be that the development of separation on an airfoil is very dependent on whether the upstream boundary layer is laminar or turbulent. Thus, the inability of the turbulence model to accurately handle transition also impacts the ability of OVERFLOW to correctly predict $c_{l,max}$. As the Reynolds number increases and the extent of laminar flow and the impact of transition on the resulting aerodynamic characteristics becomes less, the importance of being able to correctly model transition also becomes less.

All of the methods provide a reasonable prediction of the pitching-moment coefficient as it depends on angle of attack. The predictions of XFOIL and MSES are in the closest agreement to the measured values, with the XFOIL results being slightly better overall.

FLUENT Predictions

FLUENT 12.1.2 [12], which as already noted incorporates the four-equation turbulence model of Langtry and Menter [31], was released in 2009. This turbulence model is unique in having some capability of capturing the transition process. To explore this capability at lower Reynolds numbers, the E 387 was run at R = 300,000. These results are presented in Fig. 14, along with the wind-tunnel results and those of PROFIL

and OVERFLOW. For this case, FLUENT is able to account for transition to the extent that the lower corner of the low-drag range is predicted as well as it is by the codes using integral boundary-layer methods. The upper corner of the low-drag range is not captured as well as the lower limit, but it is clear that the behavior of transition is captured, especially when compared to the OVERFLOW results. The value of $c_{l,max}$ is slightly under-predicted, but is of comparable accuracy to any of the other theoretical methods. The behavior of the pitching-moment coefficient as it depends on angle of attack is predicted very well.

Selected pressure distributions as predicted using FLUENT are compared with those obtained using OVERFLOW and wind tunnel results for the E 387 at R = 300,000 in Fig. 15. The agreement between the wind-tunnel results and those from FLUENT at angles of attack of 0.0 and 4.0 degrees is exceptional. The four-equation turbulence model captures the behavior of the laminar separation bubble remarkably well, indicating that laminar separation, transition, and turbulent reattachment are all well predicted. As expected, the pressure distributions generated using OVERFLOW do not reflect any transition-dependent behavior. At an angle of attack of 8.0 degrees, FLUENT over-predicts the presence of a bubble on the upper surface near the leading edge. In the experiment, this bubble is considerably smaller and essentially disappears at an angle of attack of about 7.0 degrees, but then reappears very near the leading edge at 9.0 degrees. At stall, the pressure distributions are essentially the same; however, the angle of attack at which stall is predicted by OVERFLOW is one degree less than the experimental value, while the FLUENT prediction is 0.5 degrees greater.

To explore how the new turbulence model behaves at a higher Reynolds number, the aerodynamic characteristics of the S415 airfoil at R = 2,000,000 are predicted using FLUENT. These results are shown in Fig. 16, along with those of PROFIL, OVERFLOW, and the wind tunnel. Again, the lower corner of the low-drag region is well predicted by FLUENT. The drag coefficients in the low-drag region are also well predicted, although as was the case at the lower Reynolds number, the upper corner of the low-drag region is not predicted to be as sharp as the wind-tunnel measurements. The predicted value of $c_{l,max}$ is slightly over-predicted, while the predicted behavior of the pitching-moment coefficient with angle of attack is excellent.

Pressure distributions predicted using FLUENT for the S415 airfoil at R = 2,000,000 and several angles of attack are presented along with those of OVERFLOW and the wind tunnel in Fig. 17. At this Reynolds number, as there is little or no indication of laminar separation bubbles in the experimental results, the predicted pressure distributions from OVERFLOW and FLUENT are similar. In fact, they agree well with one another and the integrated areas agree with the experimental results, although both of the predicted distributions are shifted to slightly higher pressure coefficient values than those of the measured distributions. At $c_{l,max}$, however, the FLUENT prediction and that measured agree very well and correspond to the same critical angle of attack. As can also be observed in Fig. 16, the value of $c_{l,max}$ predicted by OVERFLOW is not only too high, it occurs at angle of attack that is over 3.0 degrees greater than that of the experiment and the FLUENT prediction.

Concluding Remarks

Based on the comparisons of the predictions of theoretical methods with measured results, it is clear the PROFIL remains an excellent design tool that is supported by a reliable and robust analysis capability. Its ability to predict drag is as good as any of the other methods, while the empirical correlation for $c_{l,max}$ is simple to apply and the most accurate of all of the predictions. While the predicted values of the pitching-moment coefficient are not as good as the XFOIL predictions, they are nevertheless reasonable. Both PROFIL and XFOIL produce reasonably good predictions of the drag. While XFOIL often over-predicts the value of $c_{l,max}$, there is no reason that an empirical correlation like that used with PROFIL could not be applied to XFOIL (and to MSES for that matter). While the ease of use of XFOIL compared to MSES encourages its use at low speeds and for single-element airfoils, MSES is necessary for higher Mach numbers and multi-element designs. With the exception of $c_{l,max}$, its predictions are comparable to those of the other boundary-layer methods. All in all, for the Reynolds-number range considered here, the predicted OVERFLOW results do not agree well with those measured.

Although only two cases were considered, the four-equation turbulence model employed in FLUENT 12.1.2 shows promise of being able to predict aerodynamics that

are strongly influenced by transitional boundary-layer behavior. With the possible exception of transition-prediction methods based on linear-stability (e^N) theory that have been "patched" into CFD methods, the new turbulence model seems to provide for an accounting of transition that has not been present thus far in CFD methods. As this new turbulence model was developed for low Reynolds number turbo-machinery applications [31], it seems likely that some work remains to better "tune" it to cover a broader range of Reynolds numbers. And while it is clear that a number of methods exist that can predict the aerodynamic characteristics of airfoils with sufficient accuracy for most engineering applications, the important consequence of being able to account for transition in Navier-Stokes solvers is not for steady two-dimensional calculations, but for three-dimensional and/or unsteady flow situations. Being able to account for transitional effects in flutter or dynamic stall predictions, for example, could have a significantly positive impact on improving the agreement between predicted aerodynamics and what actually occurs.

References

[1] Somers, D.M. and Maughmer, M.D., "Design and Experimental Results for the S406 Airfoil," Airfoils, U.S. Army Aviation Research, Development and Engineering Command, RDECOM TR 10-D-107, August 2010.

[2] Somers, D.M. and Maughmer, M.D., "Design and Experimental Results for the S407 Airfoil," U.S. Army Aviation Research, Development and Engineering Command, RDECOM TR 10-D-109, August 2010.

[3] Somers, D.M. and Maughmer, M.D., "Design and Experimental Results for the S411 Airfoil," U.S. Army Aviation Research, Development and Engineering Command, RDECOM TR 10-D-111, August 2010.

[4] Somers, D.M. and Maughmer, M.D., "Design and Experimental Results for the S414 Airfoil," U.S. Army Aviation Research, Development and Engineering Command, RDECOM TR 10-D-112, August 2010.

[5] Somers, D.M. and Maughmer, M.D., "Design and Experimental Results for the S415 Airfoil," U.S. Army Aviation Research, Development and Engineering Command, RDECOM TR 10-D-114, August 2010.

[6] Somers, D.M. and Maughmer, M.D., " Experimental Results for the E 387 Airfoil at Low Reynolds Numbers in The Pennsylvania State University Low-Speed, Low-Turbulence Wind Tunnel," U.S. Army Research, Development and Engineering Command, RDECOM TR 07-D-32, May 2007.

[7] Eppler, R., Airfoil Program System " PROFIL07," User's Guide, Richard Eppler c. 2007.

[8] Nichols, R., and Buning, P., "User's Manual for OVERFLOW 2.1, Version 2.1t.," NASA Langley Research Center, Hampton, VA, August 2008.

[9] Meakin, B. and Potsdam, M., "Reference Guide for Scalable OVERLOW-D, v1.5e," NASA Ames Research Center, Moffet Field, CA, 2002.

[10] Drela, M. and Youngren, H., "XFOIL 6.94 User Guide," Massachusetts Institute of Technology, Cambridge, MA, 2001.

[11] Drela, M., "A User's Guide to MSES 2.95," Massachusetts Institute of Technology, Cambridge, MA, 1996.

[12] "ANSYS FLUENT 12.0 Users Guide," ANSYS, Incorporated, January 2009.

[13] Brophy, C.M., "Turbulence Management and Flow Qualification of The Pennsylvania State University Low Turbulence, Low Speed, Closed Circuit Wind Tunnel," M.S. Thesis, Department of Aerospace Engineering, Penn State University, University Park, PA, 1993.

[14] Prankhurst, R.C. and Holder, D.W., Wind-Tunnel Technique, Sir Isaac Pitman & Sons, Ltd, London, 1965.

[15] Allen, H.J., and Vincenti, W.G., "Wall Interference in a Two-Dimensional-Flow Wind Tunnel, With Consideration of the Effect of Compressibility," NACA Report 782, 1944.

[16] Assessment of Experimental Uncertainty with Application to Wind Tunnel Testing, AIAA Standard S-071A-1999, Revision A of the Standard, AIAA, Reston, VA, 1999.

[17] Loving, D.L. and Katzoff, S., "The Fluorescent-Oil Film Method and Other Techniques for Boundary-Layer Flow Visualization," NASA MEMO 3-17-59L, 1959.

[18] McGhee, R.J., Beasley, W.D., and Foster, J.M., "Recent Modifications and Calibration of the Langley Low-Turbulence Pressure Tunnel," NASA TP-2328, 1984.

[19] van Ingen, J.L., Boermans, L.M.M., and Blom, J.J.H., "Low-Speed Airfoil Section Research at Delft University1of Technology," ICAS-80-10.1, Munich, October 1980.

[20] McGhee, R.J., Walker, B.S., and Millard, B.F., "Experimental Results for the Eppler 387 Airfoil at Low Reynolds Numbers in the Langley Low-Turbulence Pressure Tunnel," NASA Technical Memorandum 4062, October 1988.

[21] Volkers, D.F., "Preliminary Results of Wind-Tunnel Measurements on Some Airfoil Section Research at Delft University of Technology," ICAS-80-10.1, Munich, 1980.

[22] Althaus, D., Profilpolaren für den Modellflug, Necker-Verlag, Villingen-Schwenningen, Germany, 1980.

[23] Medina, R., "Validation of The Pennsylvania State University Low-Speed, Low-Turbulence Wind Tunnel Using Measurements of the S805 Airfoil," M.S. Thesis, Department of Aerospace Engineering, Penn State University, University Park, PA, 1994.

[24] Somers, D.M., "Design and Experimental Results for the S805 Airfoil," National Renewable Energy Laboratory, NREL Report No. SR-440-6917, October 1988.

[25] Braslow, A.L. and Knox, E.C., "Simplified Method for Determination of Critical Height of Distributed Roughness Particles for Boundary-Layer Transition at Mach Numbers From 0 to 5," NACA TN 4363, 1958.

[26] Abbott, I.H., von Doenhoff, A.E., and Stivers, L.S., Jr., Summary of Airfoil Data, NACA Report 824, 1945. (Supersedes NACA WR L-560).

[27] Drela, M., Giles, M.B., "Viscous-Inviscid Analysis of Transonic and Low Reynolds Number Airfoils," AIAA Journal, Vol. 25, No. 10, October 1987.

[28] Drela, M., "Implicit Implementation of the Full e^n Transition Criterion," AIAA Paper 2003-4066, 21st Applied Aerodynamics Conference, Orlando, Florida, June 2003.

[29] Chan, W.M., Rogers, S.E., Nash, S.M., Buning, P.G., Meakin, R.L, Boger, D.A., Pandya, S., "Chimera Grid Tools User's Manual, Version 2.0," NASA Ames Research Center, July 2007.

[30] Chan, W.M., Gomez, R.J., Rogers, S.E. and Buning, P.G., "Best Practices in Overset Grid Generation," AIAA Paper 2002-3191, 32nd AIAA Fluid Dynamics Conference, St. Louis, Missouri, June 2002.

[31] Langtry, R.B., Menter, F.R., "Correlation-Based Transition Modeling for Unstructured Parallelized Computational Fluid Dynamics Codes," AIAA Journal, Vol. 47, No. 12, December 2009, pp 2894-2906.

[32] "GAMBIT Modeling Guide," Fluent, Inc, November 1999.

[33] Somers, D.M., "The S415 and S418 Airfoils," U.S. Army Aviation Research, Development and Engineering Command, RDECOM TR 10-D-113, August 2010.

[34] Rumsey, C.L., "Apparent Transition Behavior of Widely-Used Turbulence Models," AIAA Paper 2006-3906, 36th AIAA Fluid Dynamics Conference and Exhibit, San Francisco, California, June 2006.

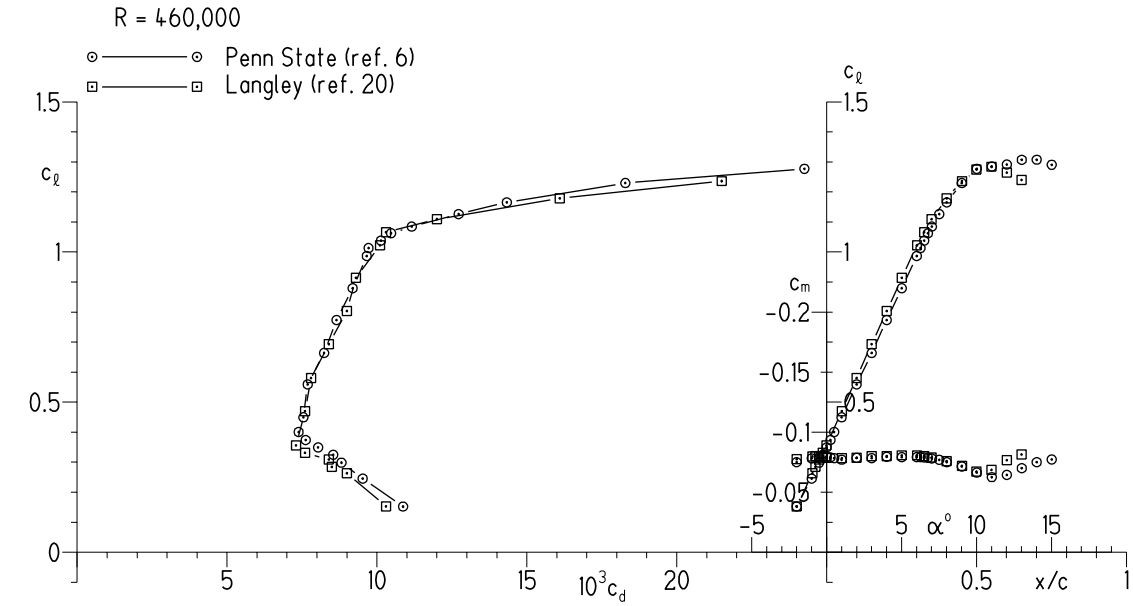

(a) R = 460,000

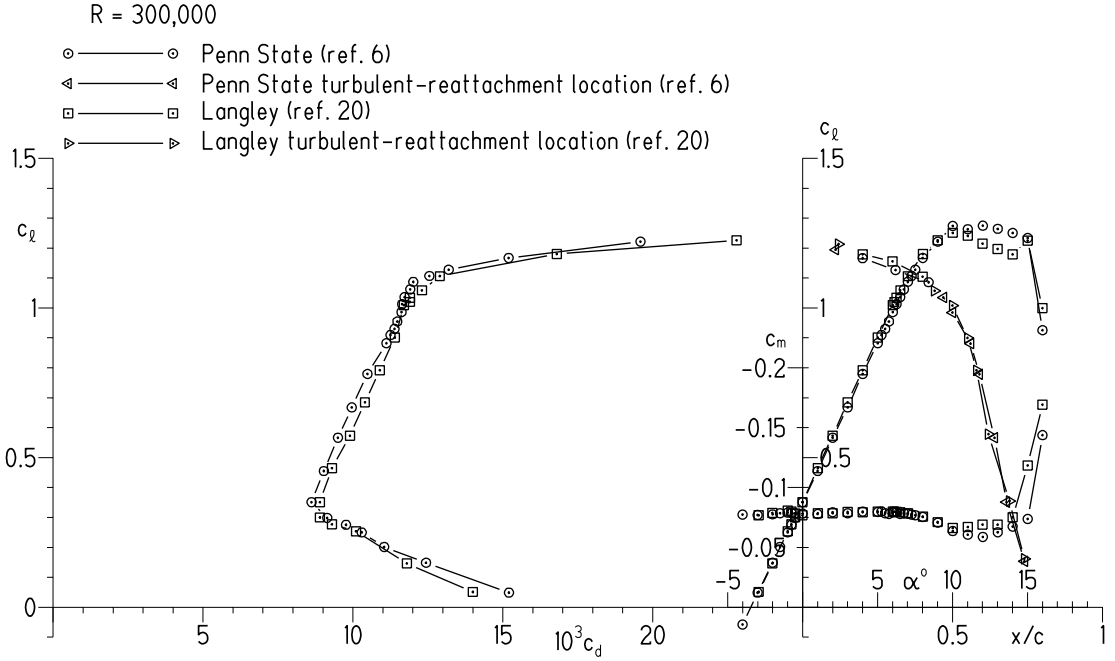

(b) R = 300,000

Fig. 1 Aerodynamic characteristics of the E 387 airfoil measured at Penn State compared with those measured in other wind tunnels.

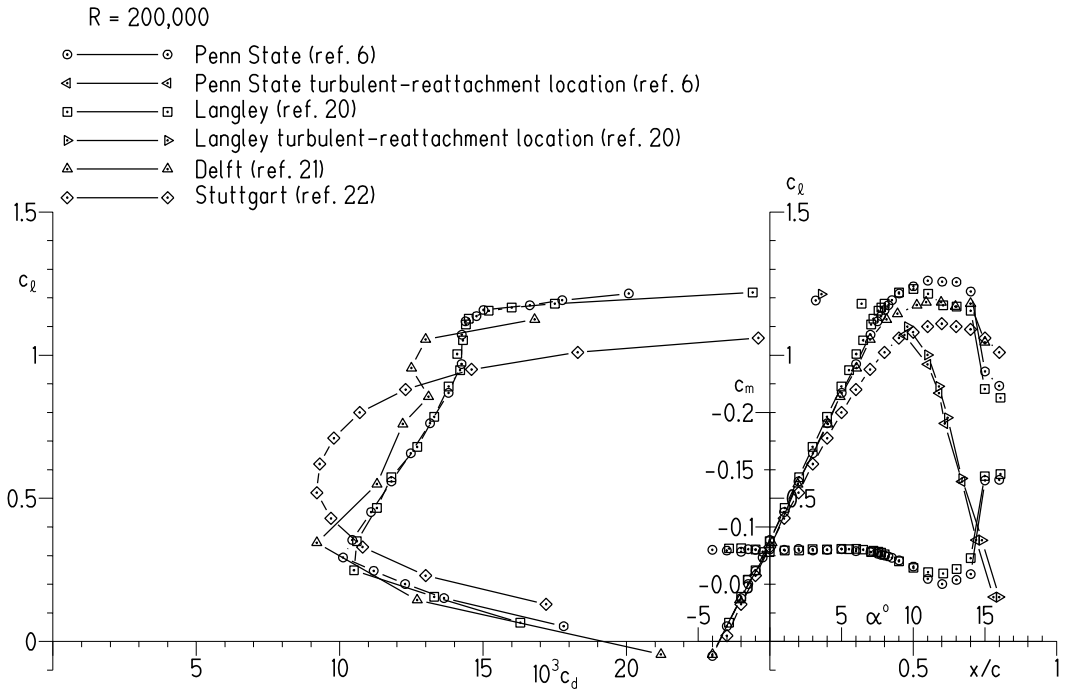

(c) R = 200,000

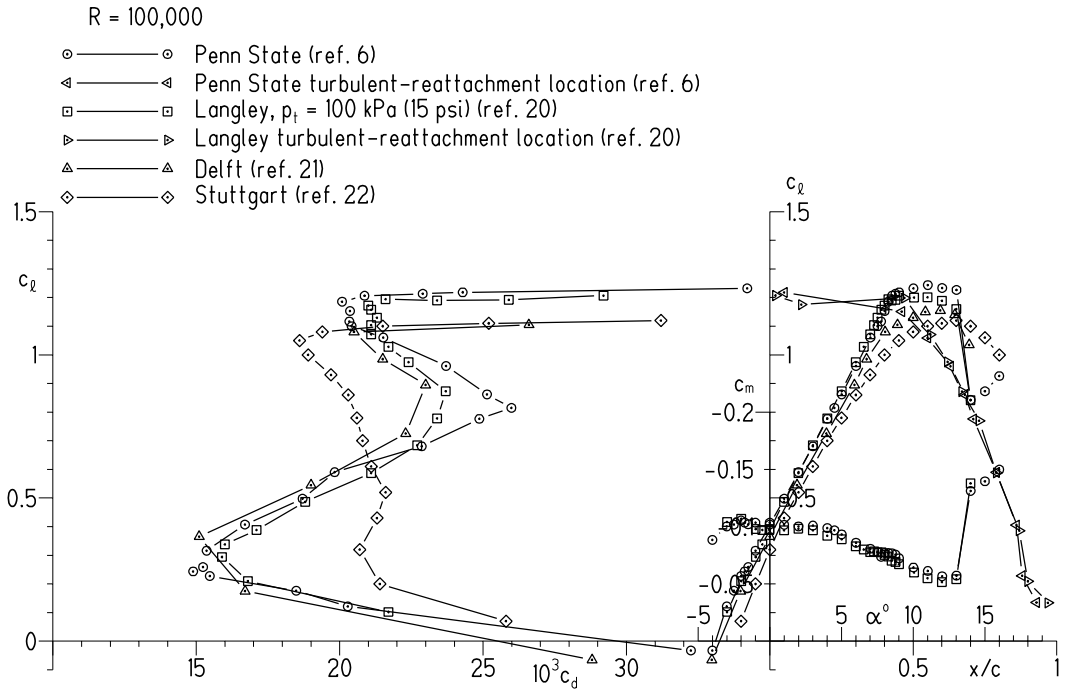

(d) R = 100,000

Fig. 1 - Continued

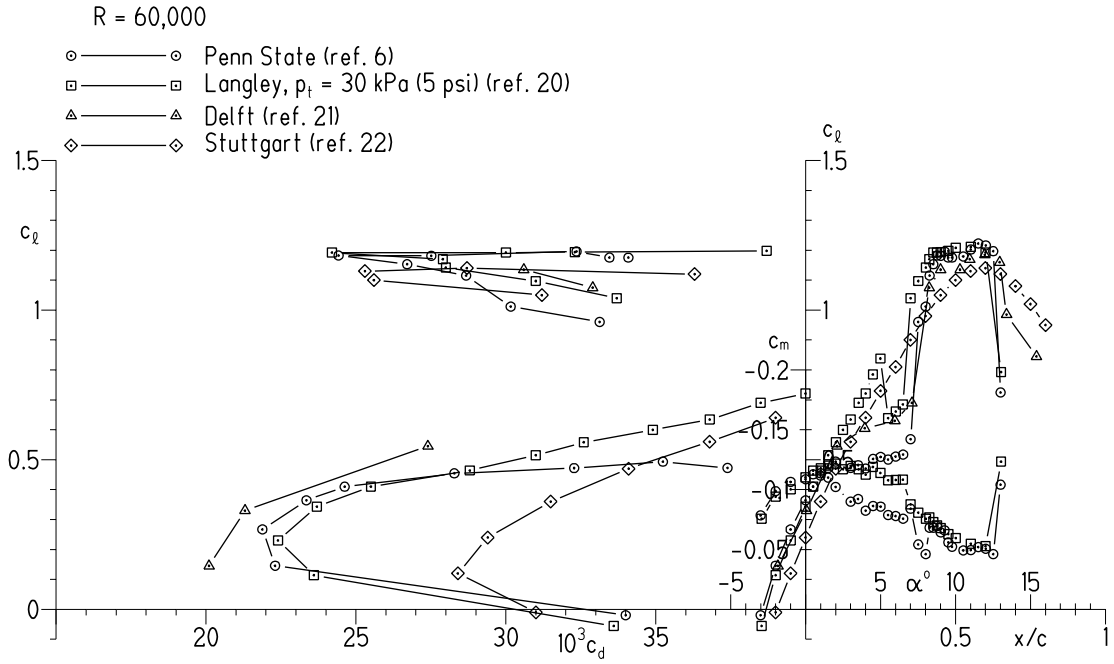

(e) R = 60,000

Fig. 1 - Concluded

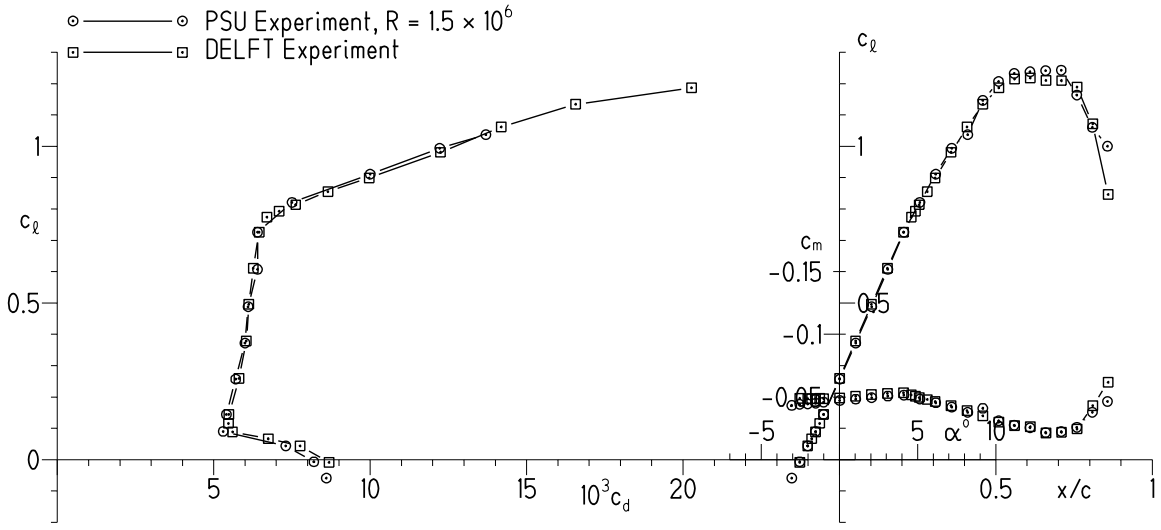

(a) R = 1,500,000

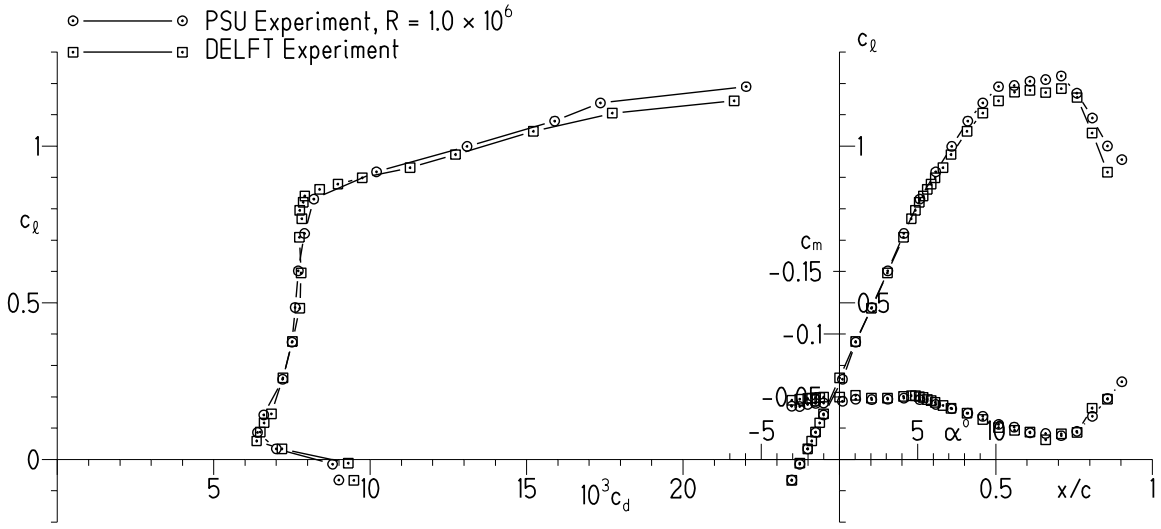

(b) R = 1,000,000

Fig. 2 Aerodynamic characteristics of the S805 airfoil measured at Penn State compared with those measured at Delft.

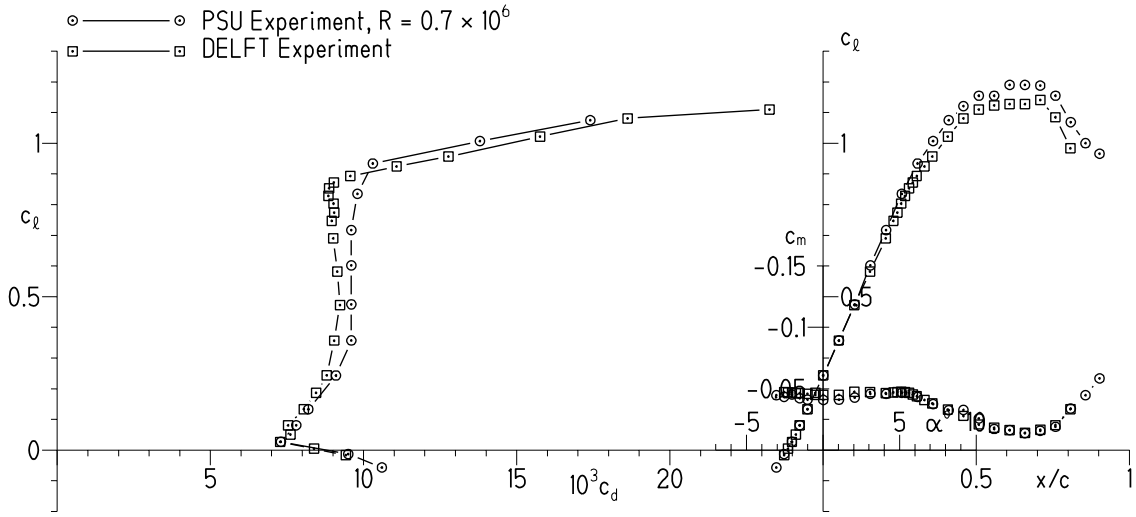

(c) R = 700,000

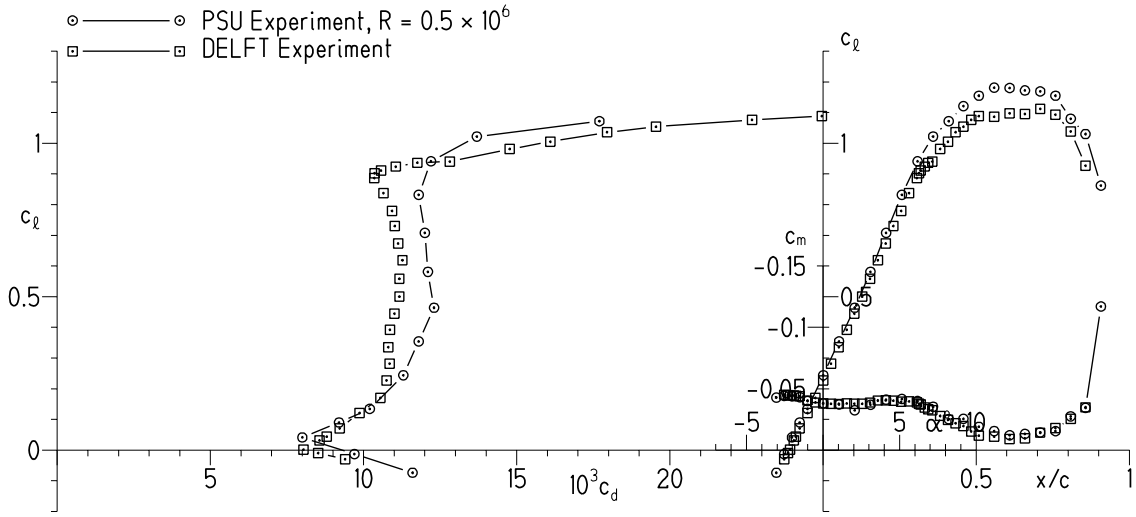

(d) R = 500,000

Fig. 2 - Concluded

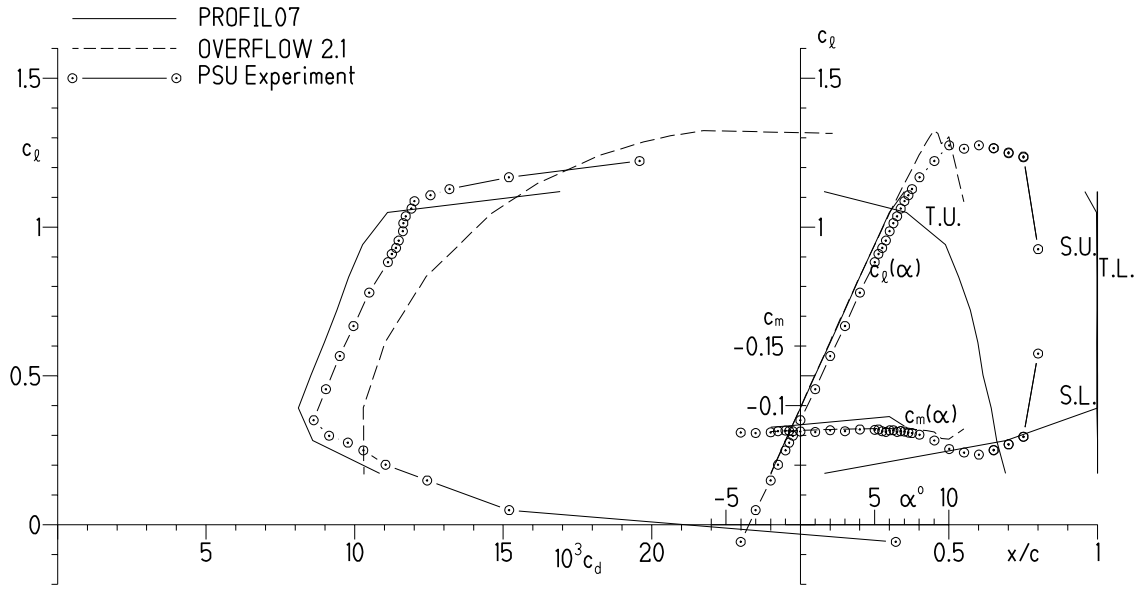

(a) PROFIL7, OVERFLOW, and Penn State experimental results.

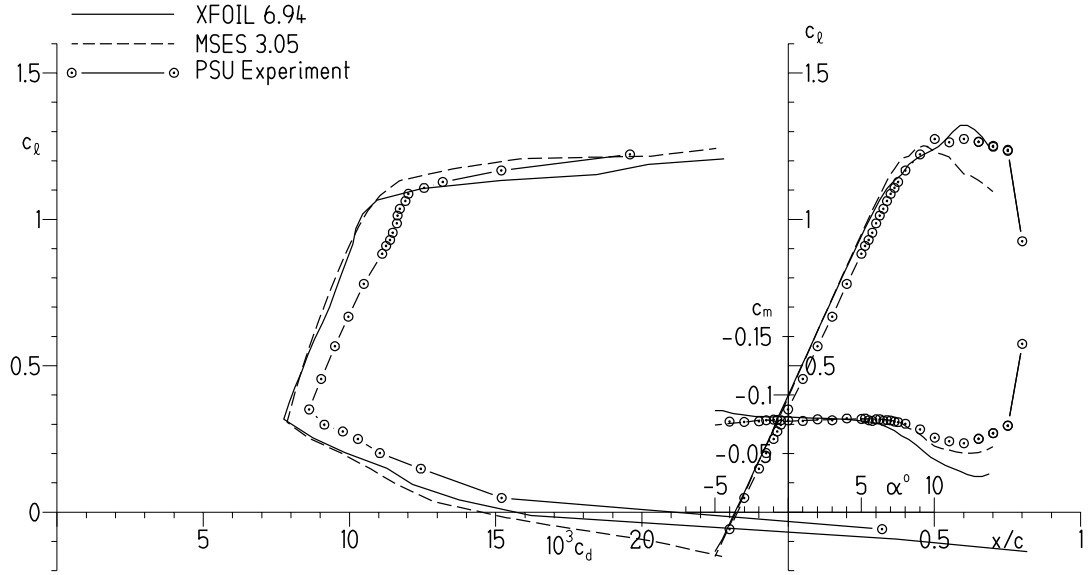

(b) XFOIL, MSES, and Penn State experimental results.

Fig. 3 Comparison of predicted and measured aerodynamic characteristics for the E 387 airfoil, R = 300,000.

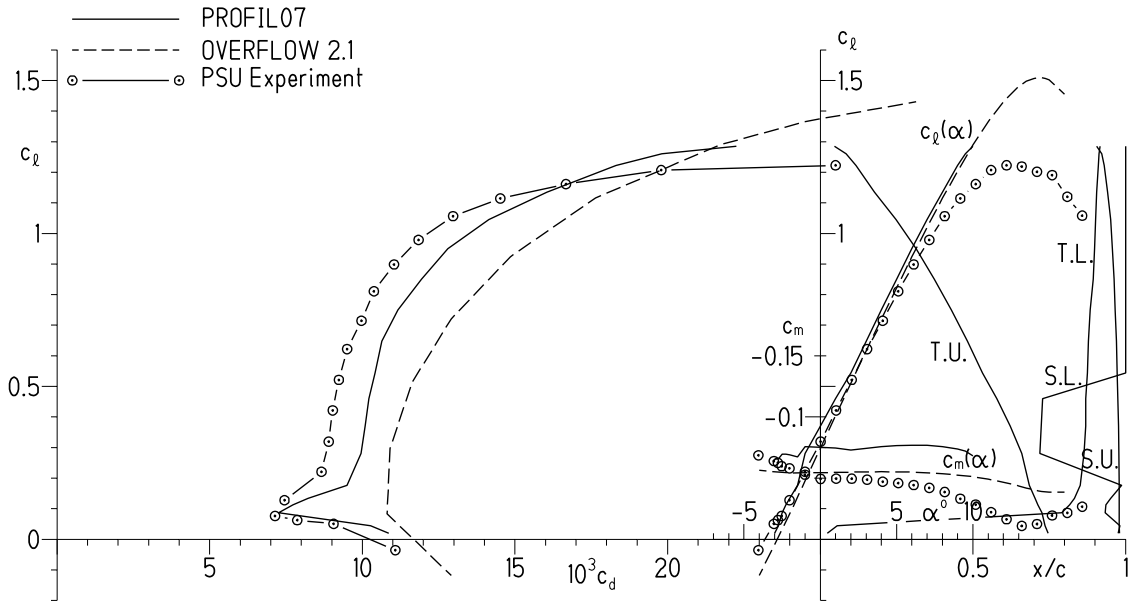

(a) PROFIL7, OVERFLOW, and Penn State experimental results.

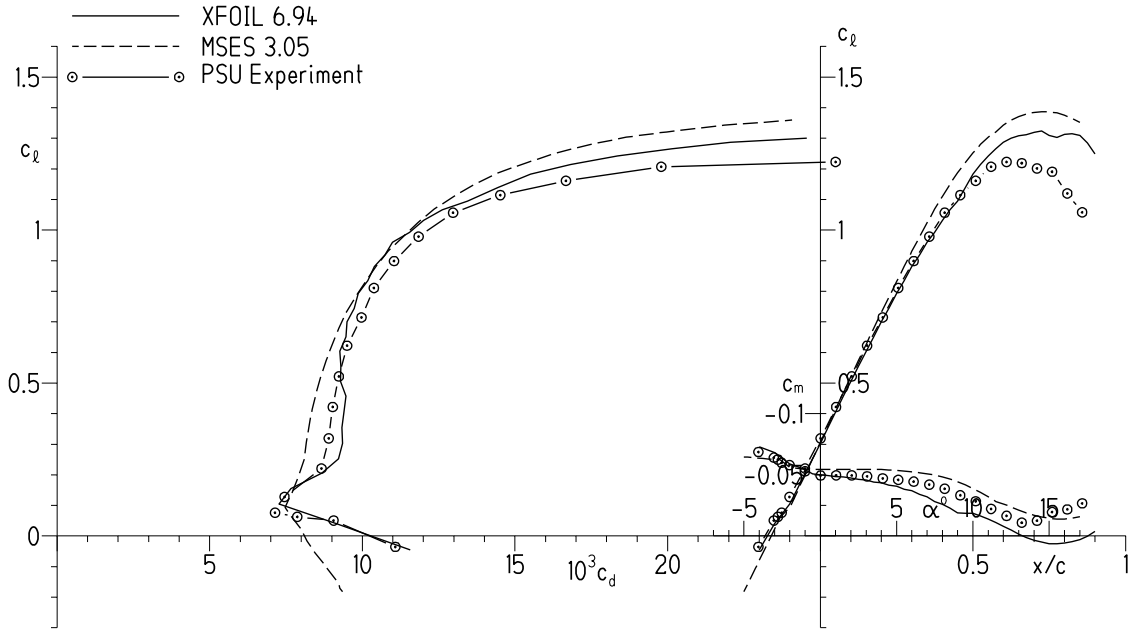

(b) XFOIL, MSES, and Penn State experimental results.

Fig. 4 Comparison of predicted and measured aerodynamic characteristics for the S406 airfoil, R = 500,000.

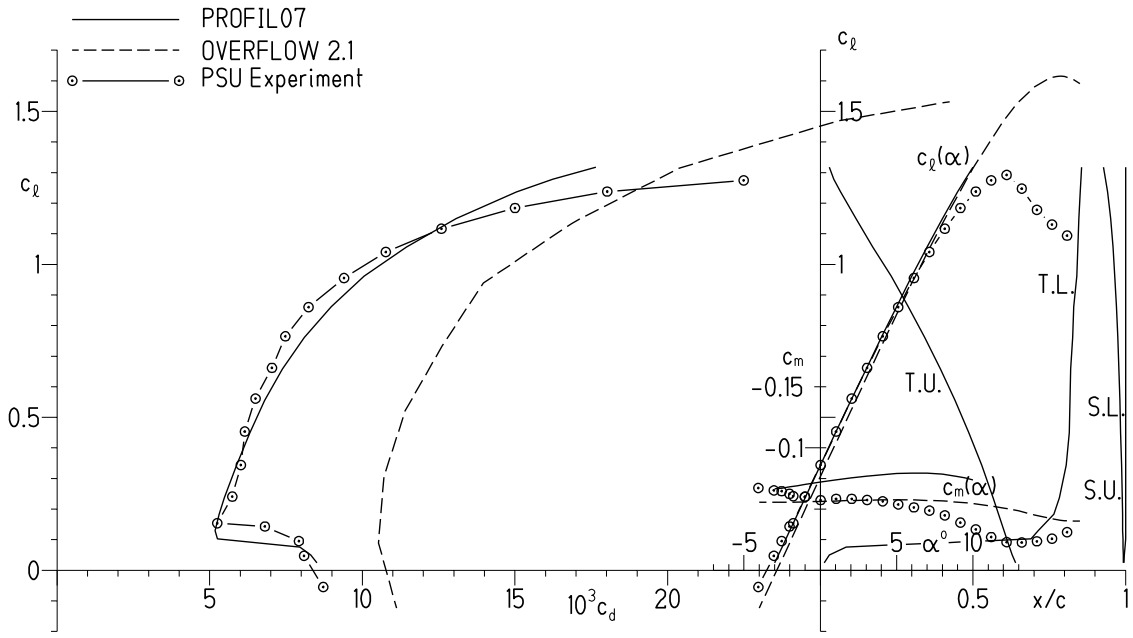

(a) PROFIL7, OVERFLOW, and Penn State experimental results.

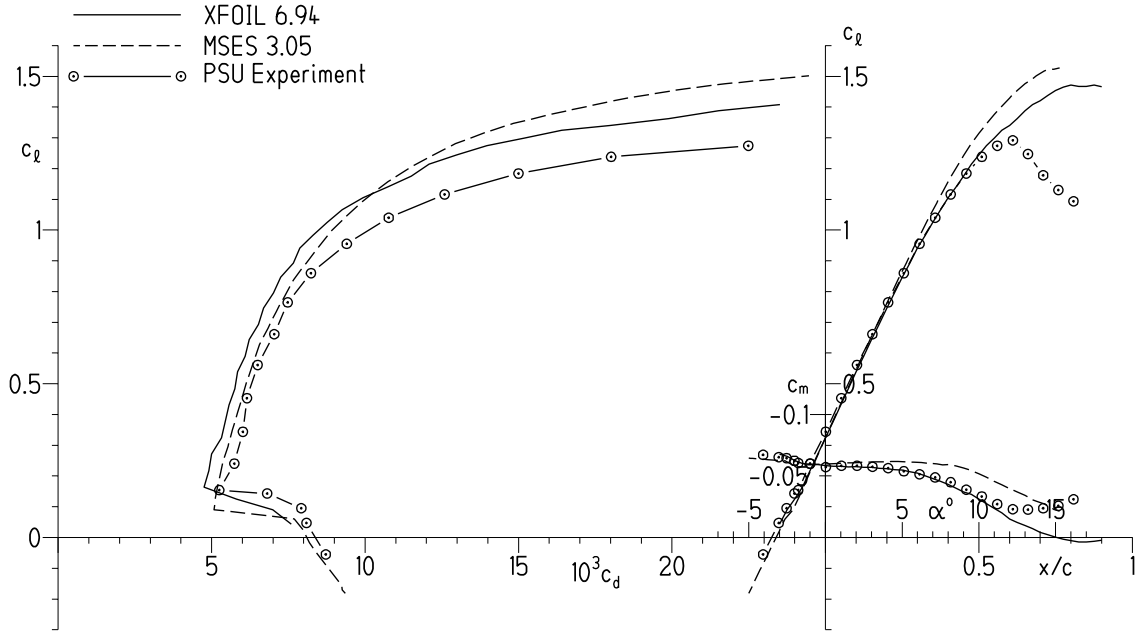

(b) XFOIL, MSES, and Penn State experimental results.

Fig. 5 Comparison of predicted and measured aerodynamic characteristics for the S406 airfoil, R = 1,500,000.

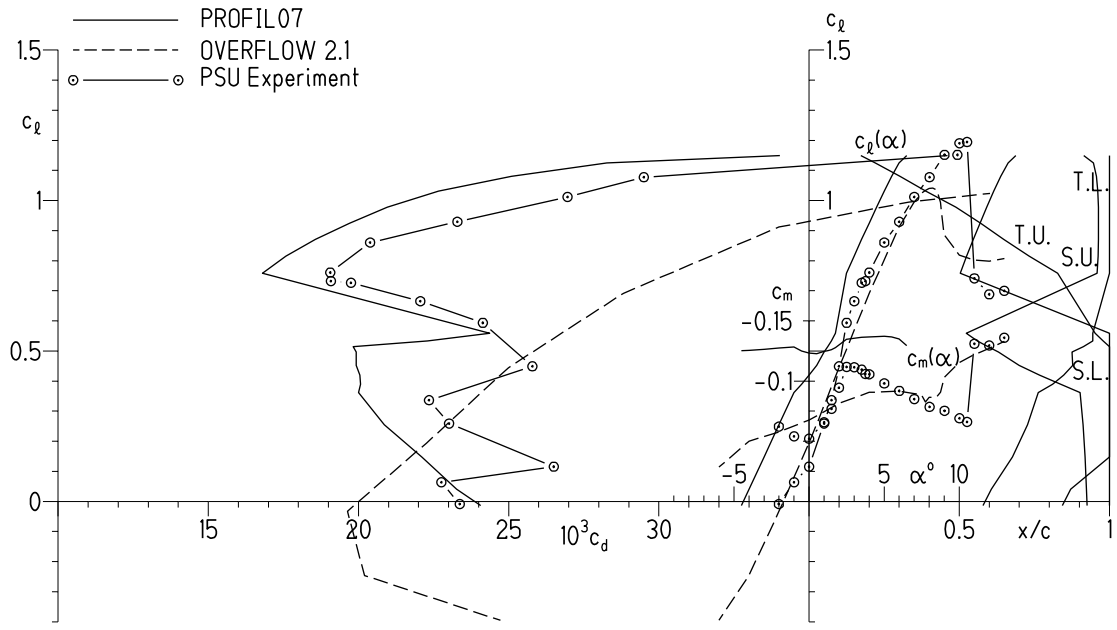

(a) PROFIL7, OVERFLOW, and Penn State experimental results.

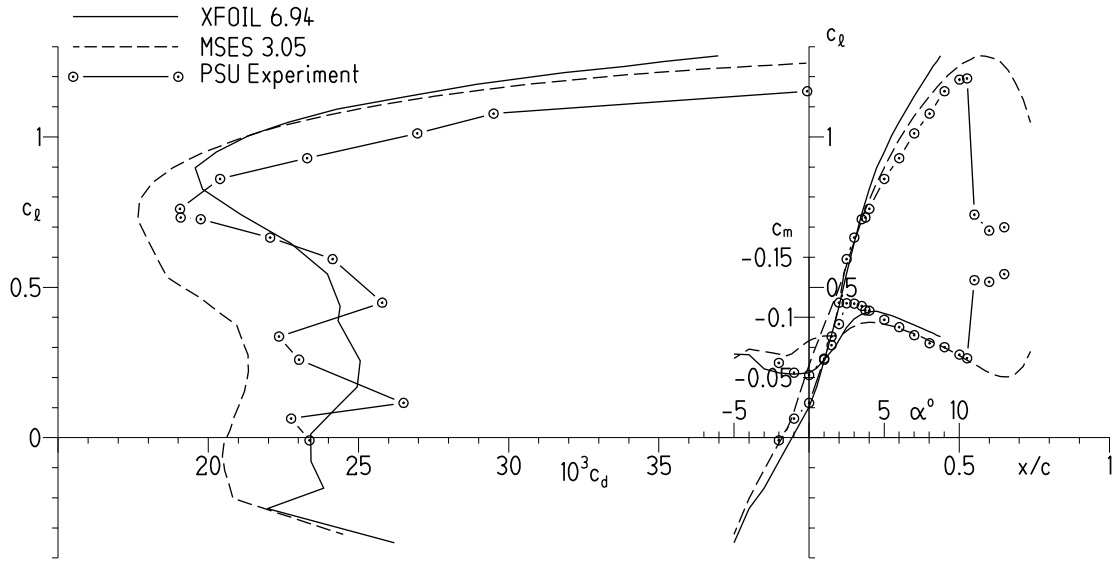

(b) XFOIL, MSES, and Penn State experimental results.

Fig. 6 Comparison of predicted and measured aerodynamic characteristics for the S407 airfoil, R = 70,000.

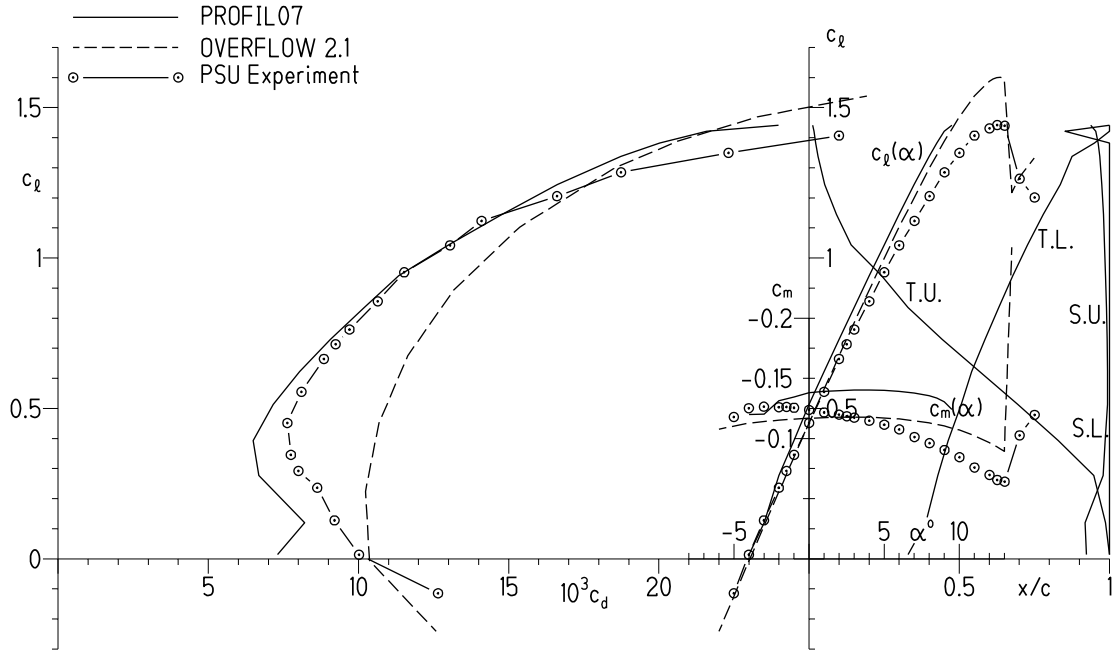

(a) PROFIL7, OVERFLOW, and Penn State experimental results.

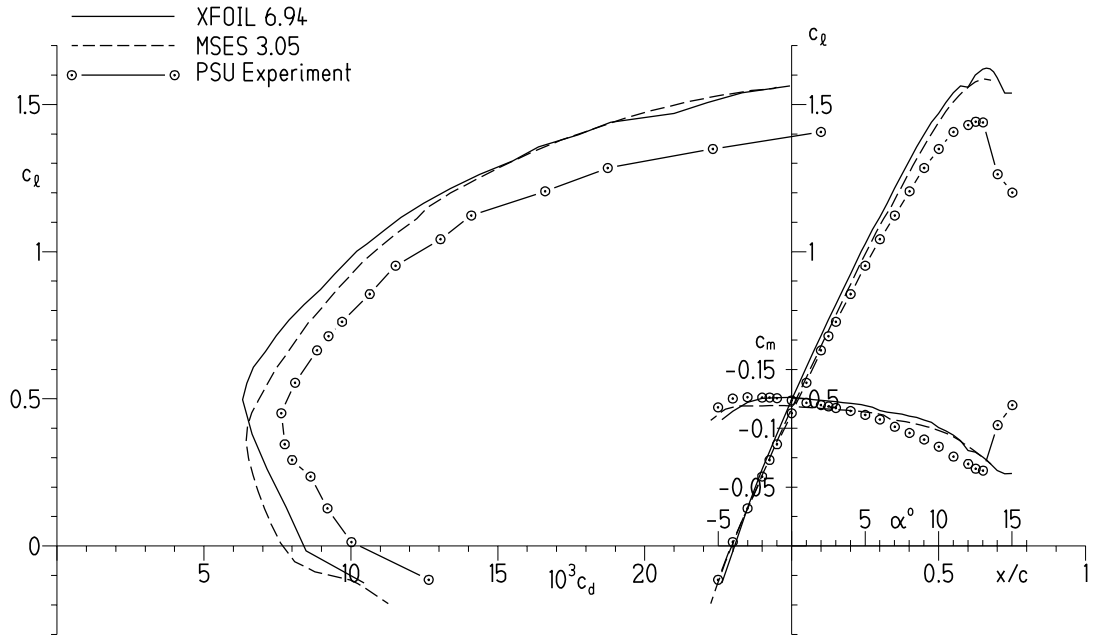

(b) XFOIL, MSES, and Penn State experimental results.

Fig. 7 Comparison of predicted and measured aerodynamic characteristics for the S407 airfoil, R = 600,000.

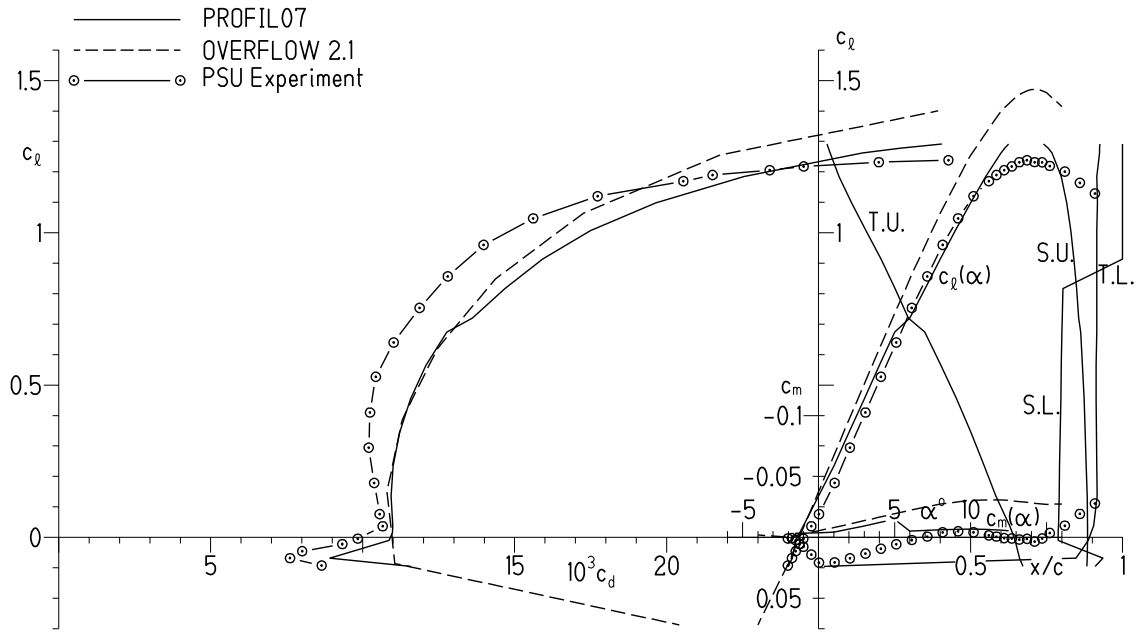

(a) PROFIL7, OVERFLOW, and Penn State experimental results.

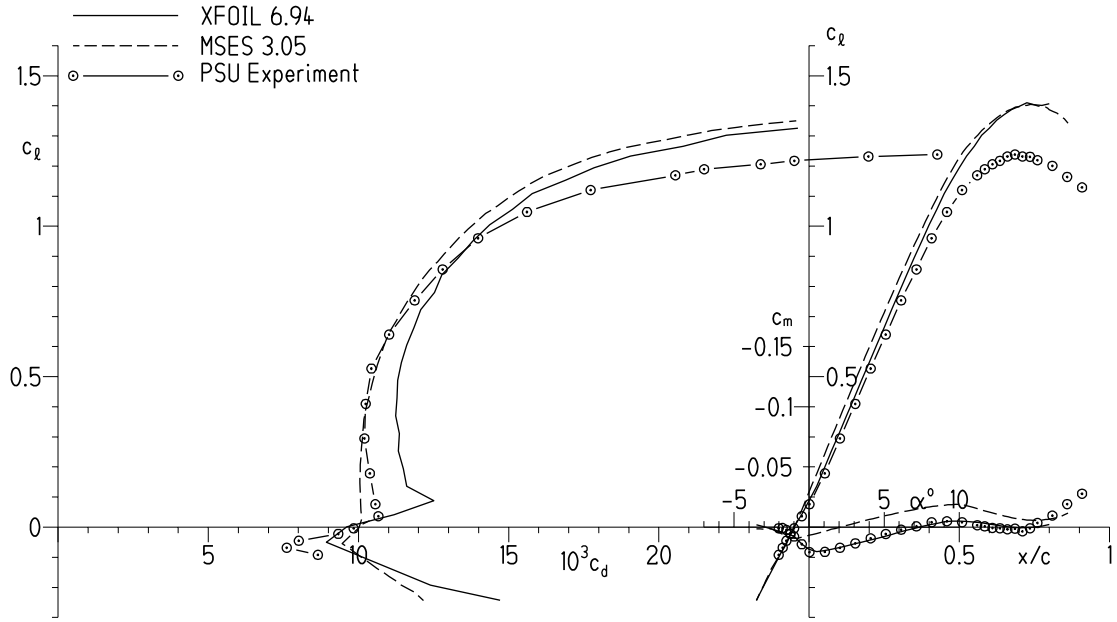

(b) XFOIL, MSES, and Penn State experimental results.

Fig. 8 Comparison of predicted and measured aerodynamic characteristics for the S411 airfoil, R = 500,000.

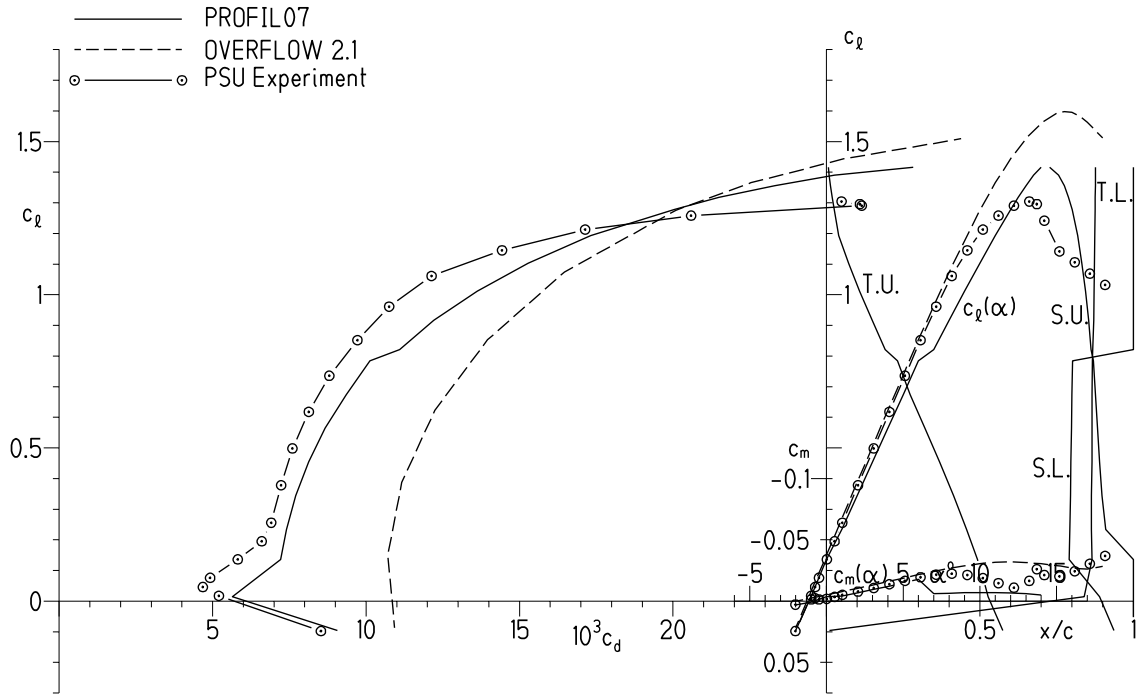

(a) PROFIL7, OVERFLOW, and Penn State experimental results.

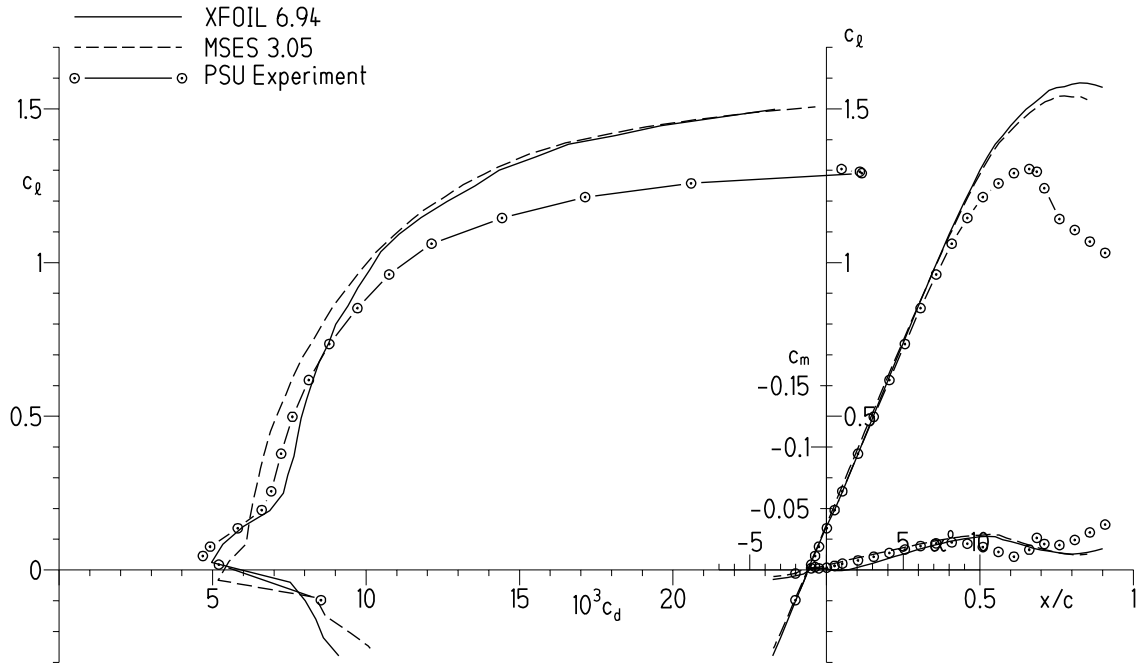

(b) XFOIL, MSES, and Penn State experimental results.

Fig. 9 Comparison of predicted and measured aerodynamic characteristics for the S411 airfoil, R = 1,500,000.

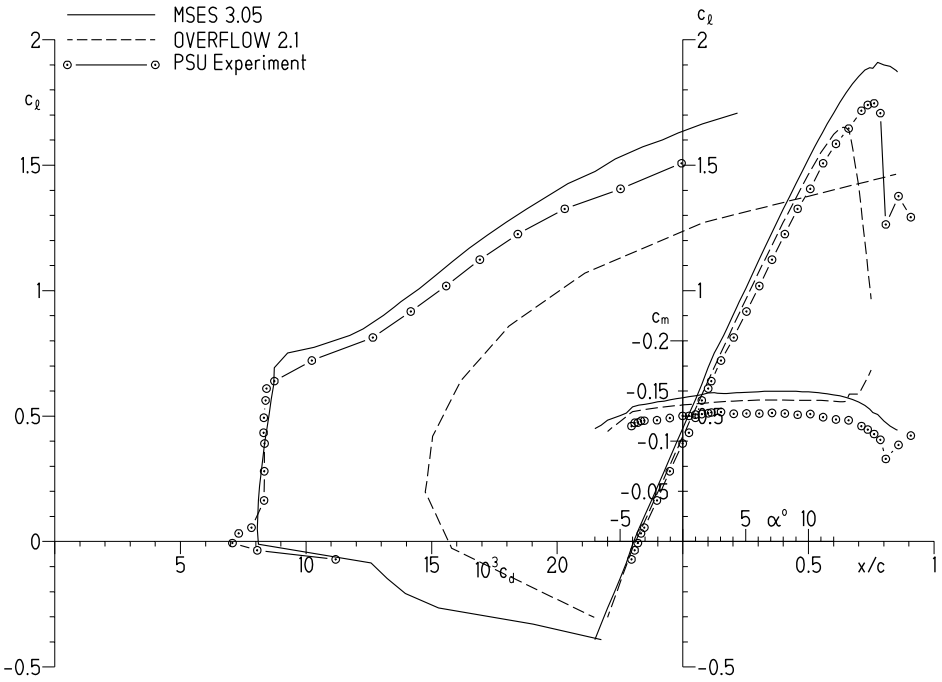

Fig. 10 Comparison of MSES and OVERFLOW predictions and measured aerodynamic characteristics for the S414 airfoil, R = 700,000.

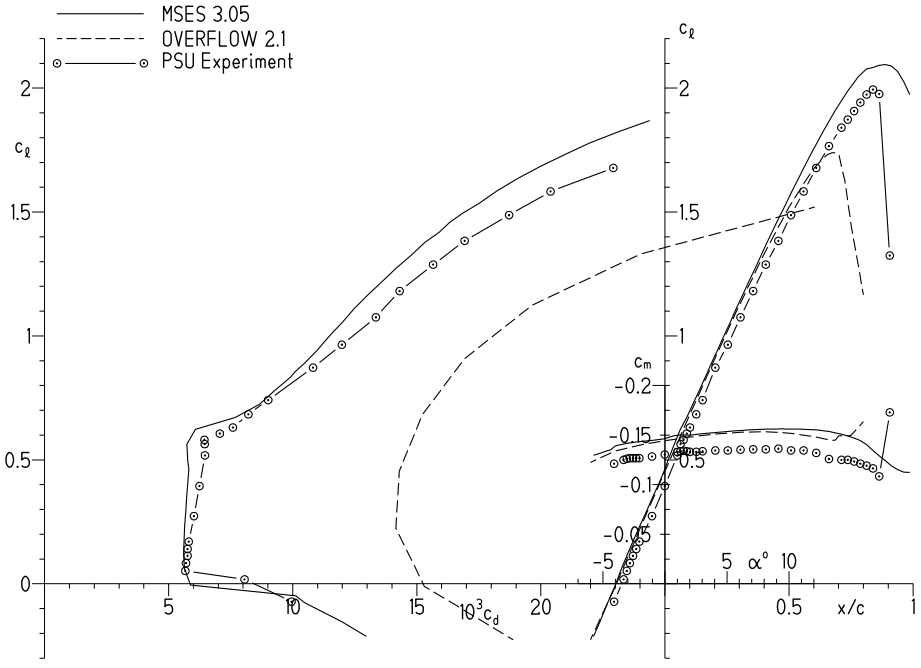

Fig. 11 Comparison of MSES and OVERFLOW predictions and measured aerodynamic characteristics for the S414 airfoil, R = 1,500,000.

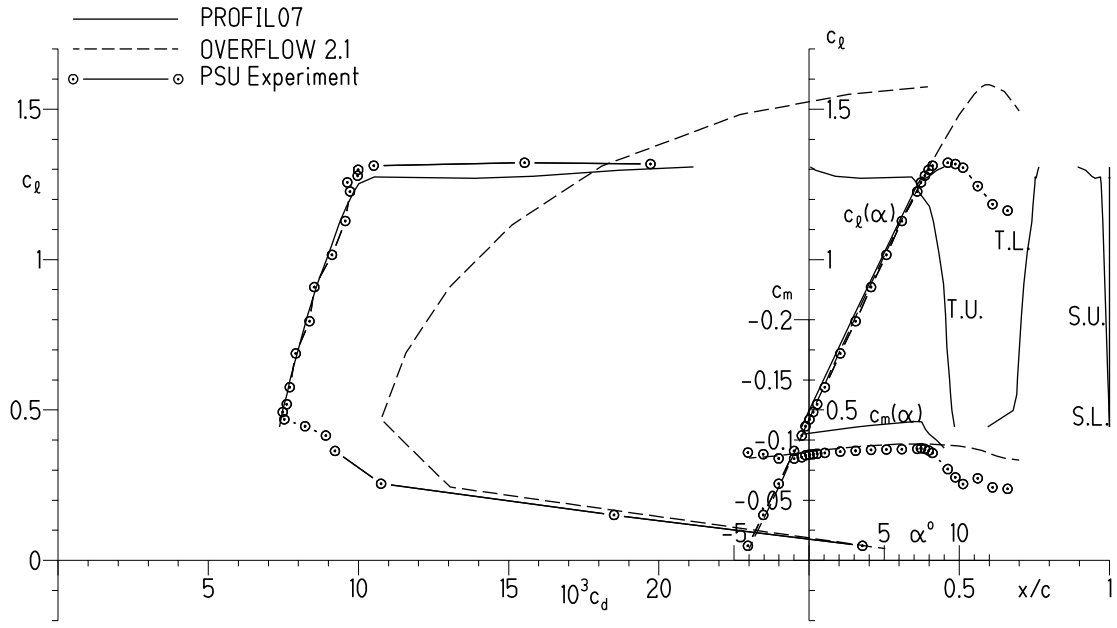

(a) PROFIL7, OVERFLOW, and Penn State experimental results.

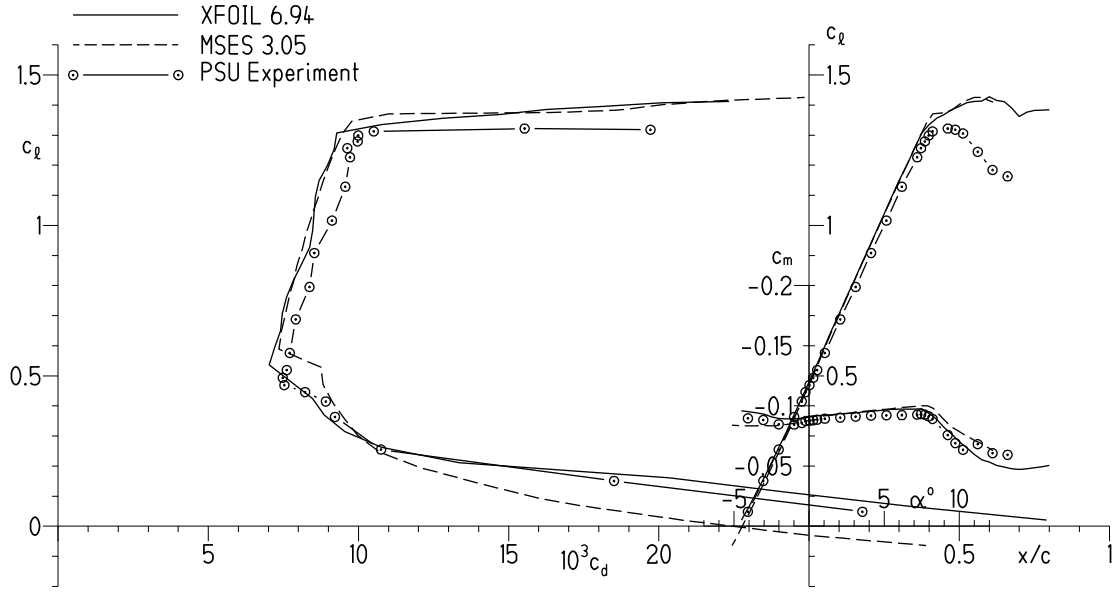

(b) XFOIL, MSES, and Penn State experimental results.

Fig. 12 Comparison of predicted and measured aerodynamic characteristics for the S415 airfoil, R = 1,000,000.

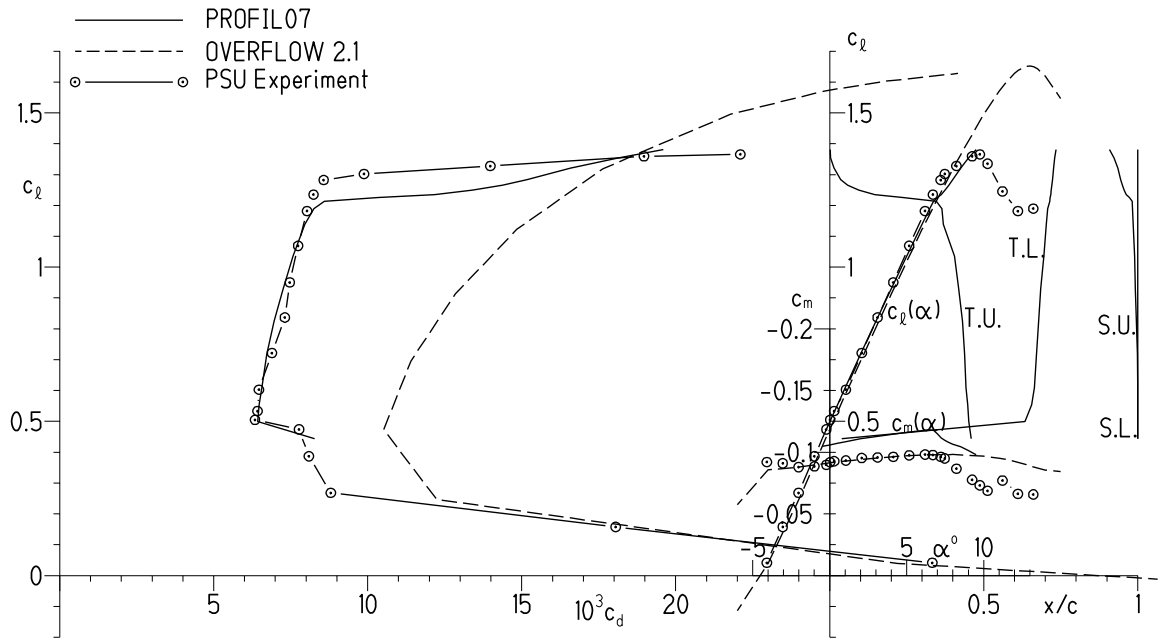

(a) PROFIL7, OVERFLOW, and Penn State experimental results.

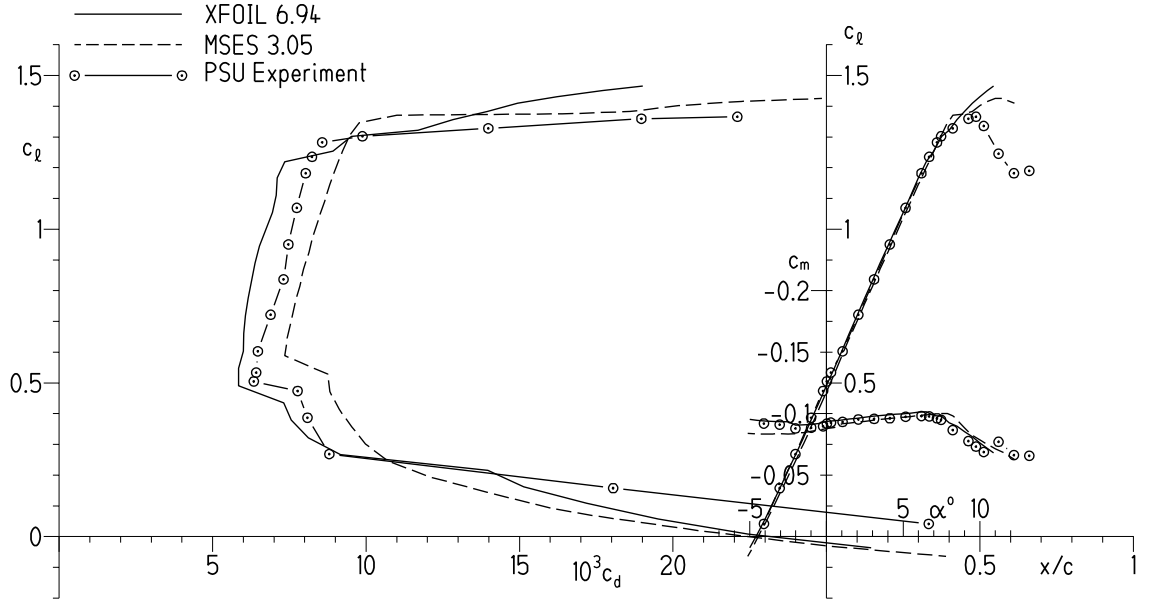

(b) XFOIL, MSES, and Penn State experimental results.

Fig. 13 Comparison of predicted and measured aerodynamic characteristics for the S415 airfoil, R = 2,000,000.

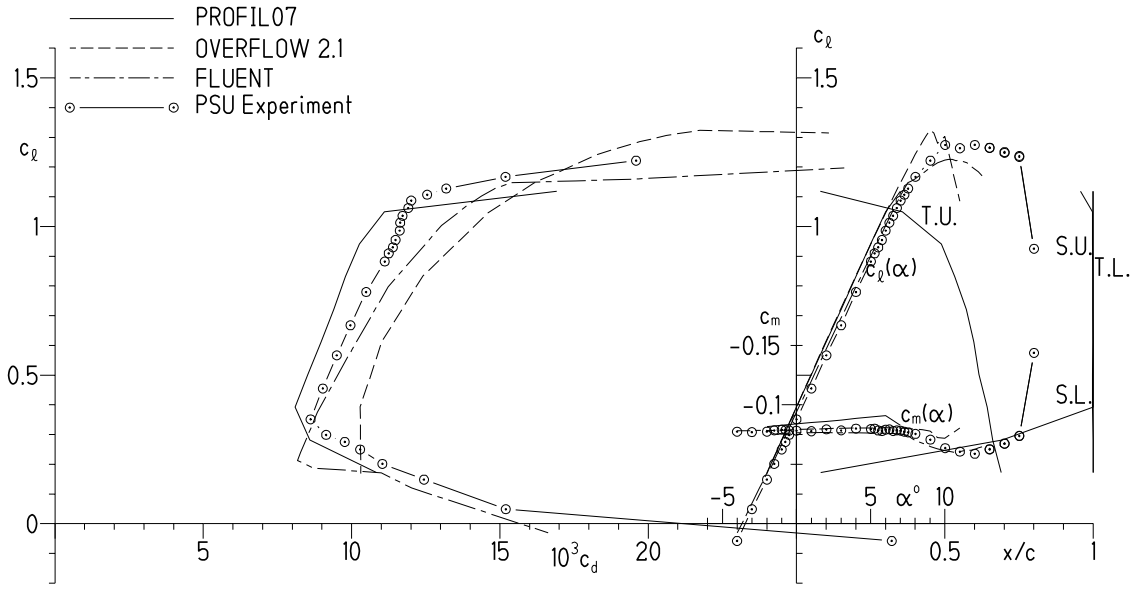

Fig. 14 Comparison of predicted and measured aerodynamic characteristics for the E 387 airfoil, R = 300,000

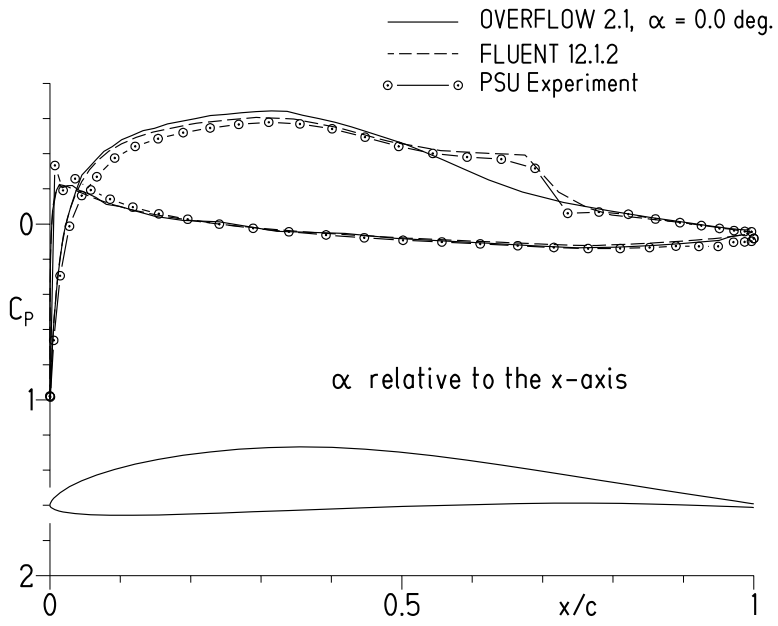

(a) α = 0.0 deg.

Fig. 15 Comparison of E 387 airfoil theoretical and experimental pressure distributions for R = 300,000.

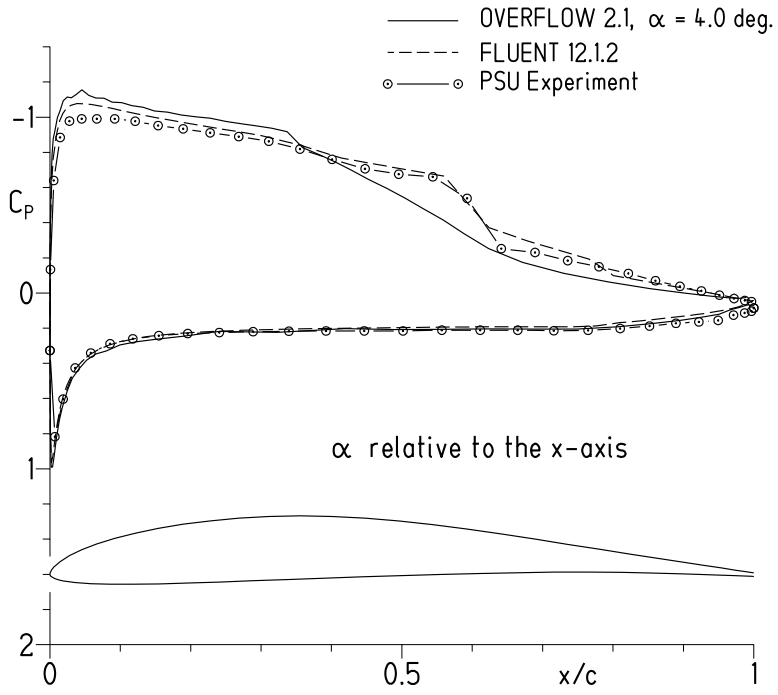

(b) α = 4.0 deg.

Fig. 15 - Continued

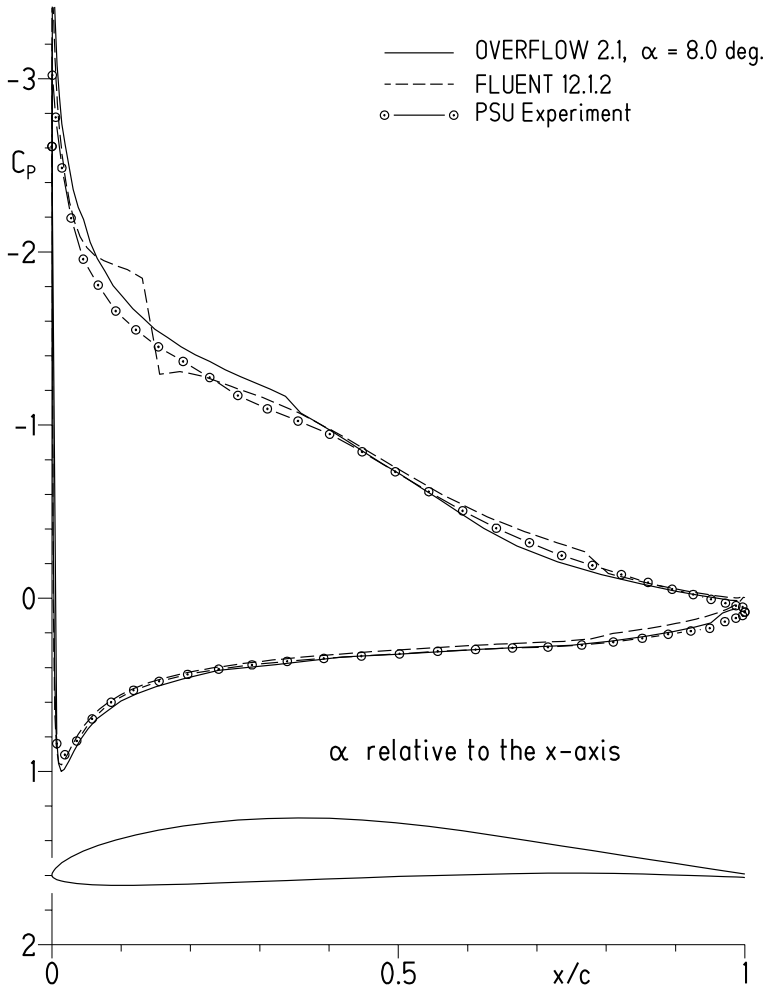

(c) $\alpha = 8.0$ deg.

Fig. 15 - Continued

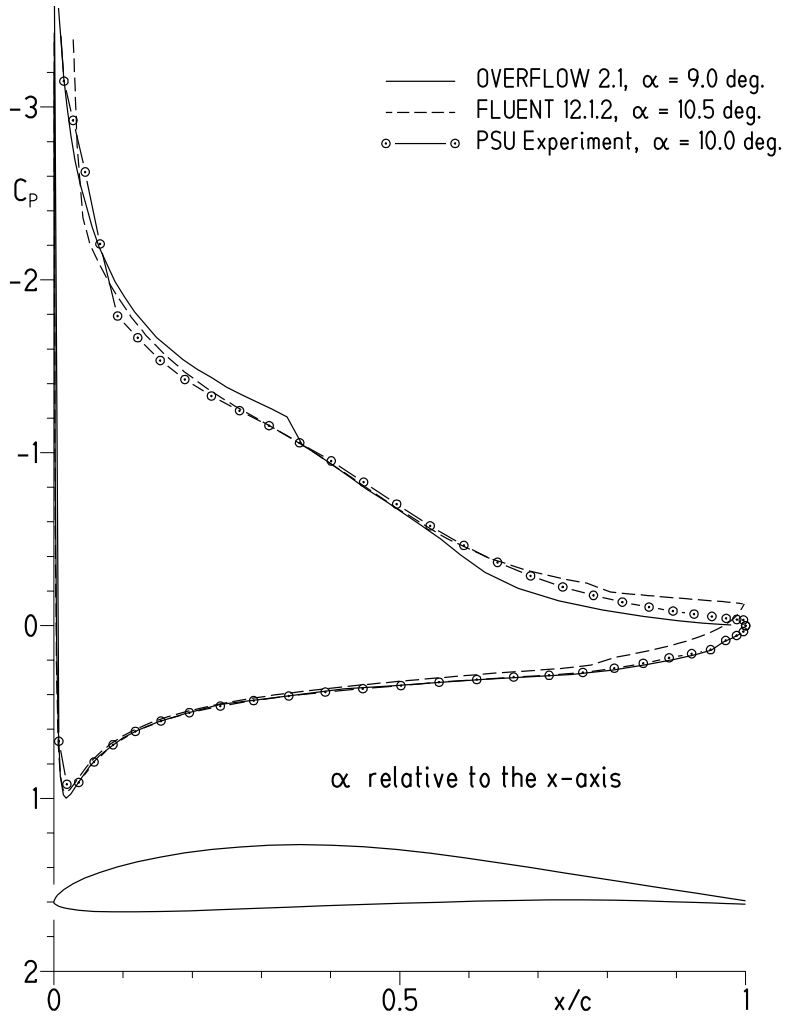

(d) Angle of attack for $c_{l,max}$.

Fig. 15 - Concluded

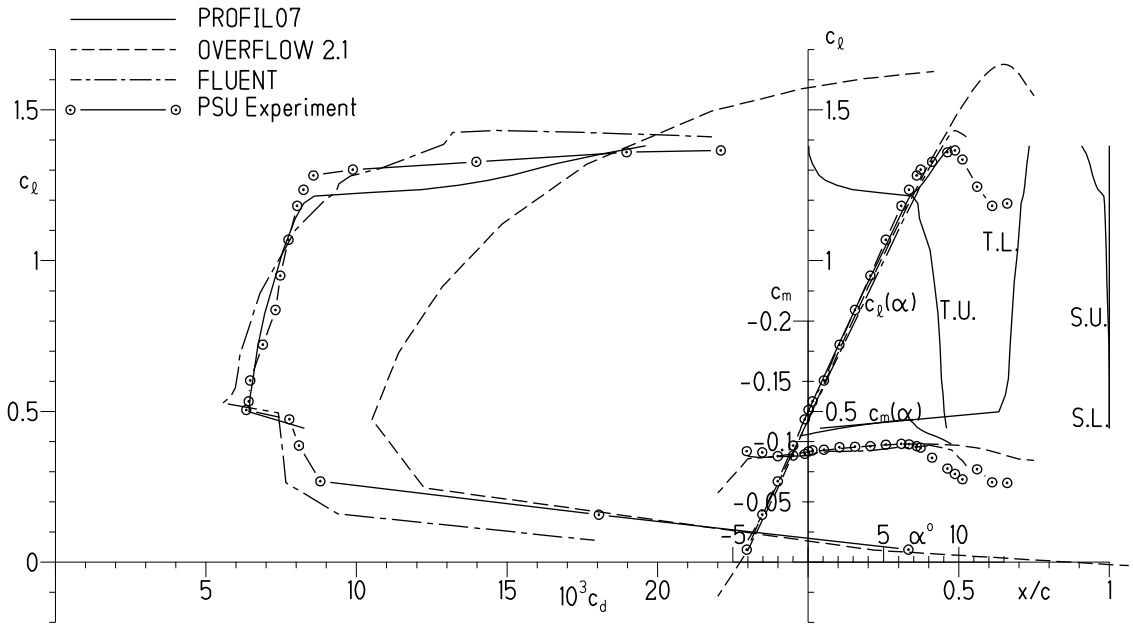

Fig. 16 Comparison of predicted and measured aerodynamic characteristics for the S415 airfoil, R = 2,000,000.

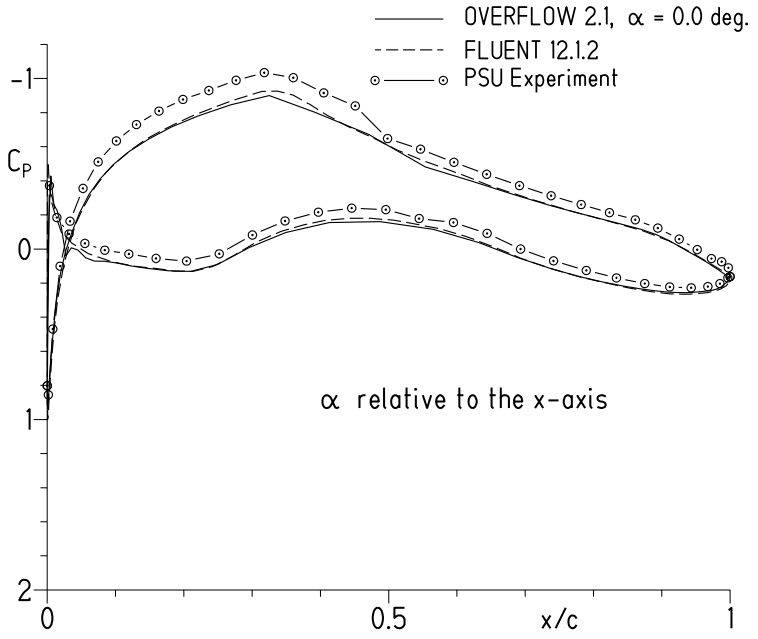

(a) $\alpha = 0.0$ deg.

Fig. 17 Comparison of S415 airfoil theoretical and experimental pressure distributions for R = 2,000,000.

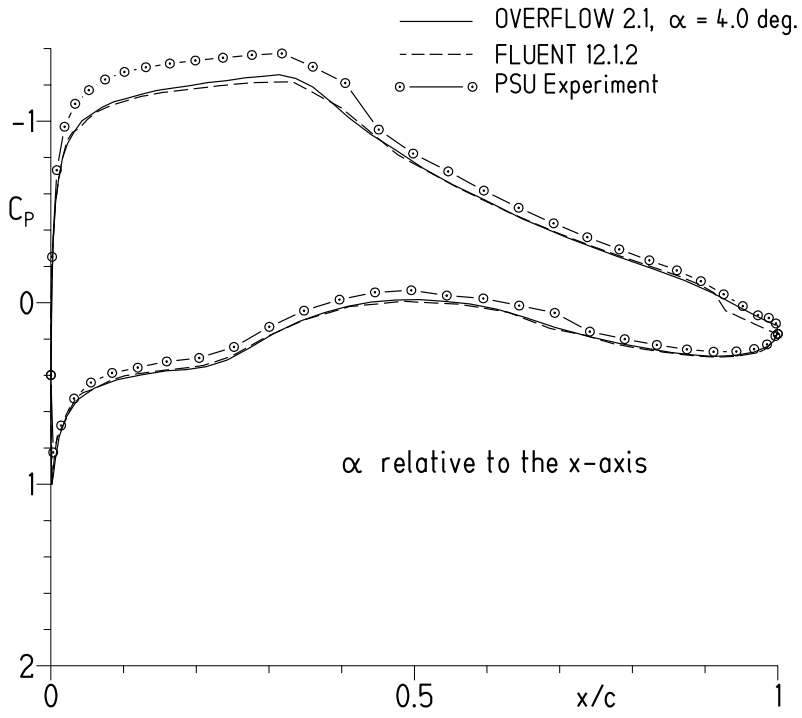

(b) $\alpha = 4.0$ deg.

Fig. 17 - Continued

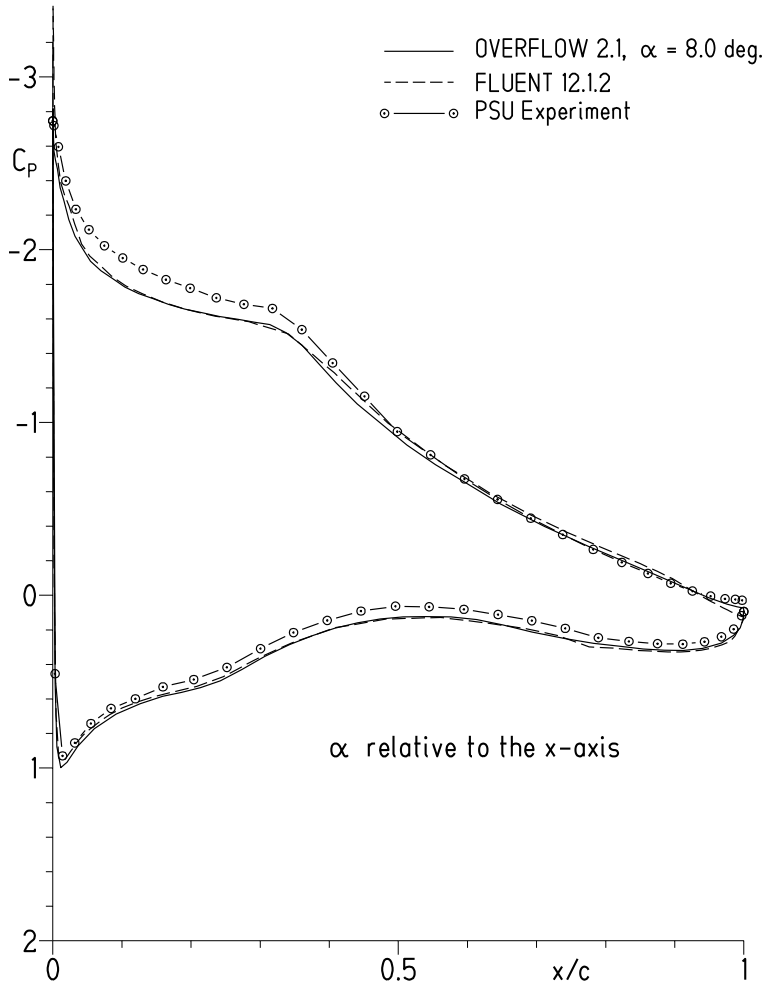

(c) $\alpha = 8.0$ deg.

Fig. 17 - Continued

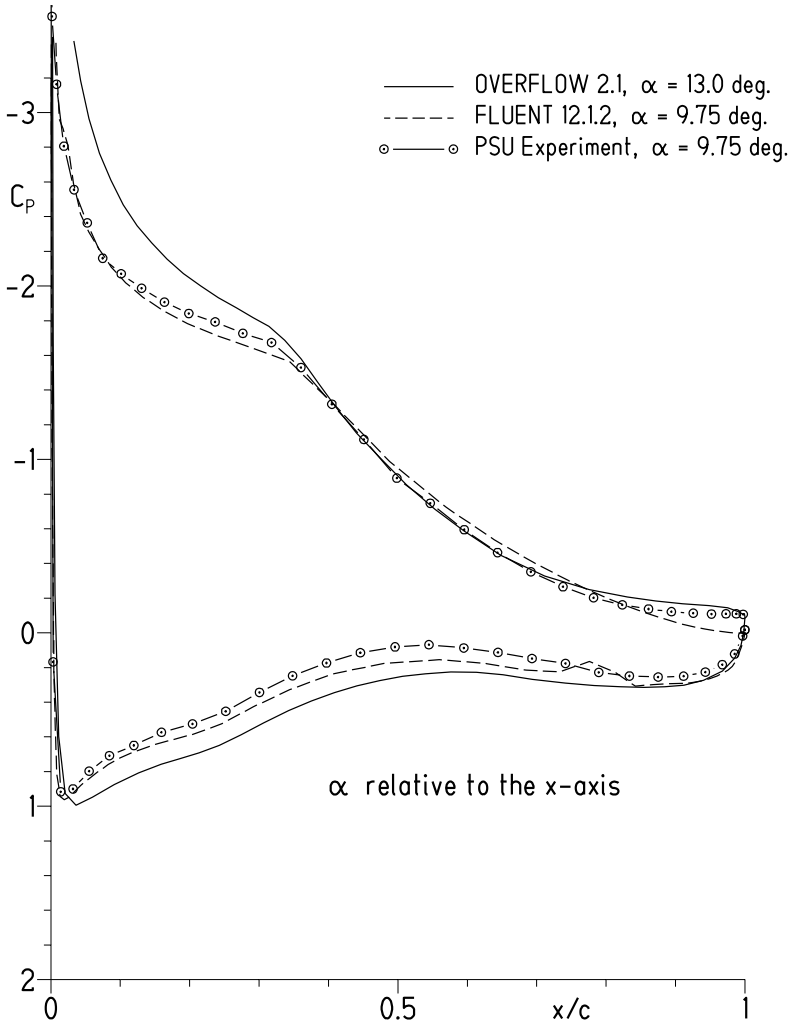

(d) Angle of attack for $c_{l,max}$.

Fig. 17 - Concluded

REPORT DOCUMENTATION PAGE

Form Approved
OMB No. 0704-0188

1. REPORT DATE *(DD-MM-YYYY)*	2. REPORT TYPE	3. DATES COVERED *(From - To)*
xx-08-2010	FINAL REPORT	Sep 2007 - Jun 2010

4. TITLE AND SUBTITLE

Comparisons of Theoretical Methods for Predicting Airfoil Aerodynamic Characteristics

5a. CONTRACT NUMBER
W911W6-07-C-0047

5b. GRANT NUMBER

5c. PROGRAM ELEMENT NUMBER

6. AUTHOR(S)

Maughmer, Mark D. and Coder, James G.

5d. PROJECT NUMBER

5e. TASK NUMBER

5f. WORK UNIT NUMBER

7. PERFORMING ORGANIZATION NAME(S) AND ADDRESS(ES)

Airfoils, Incorporated
Attn: Dan M. Somers
122 Rose Drive
Port Matilda PA 16870-7535

8. PERFORMING ORGANIZATION REPORT NUMBER

SBIR Topic Number A06-006
Proposal Number A2-2972

9. SPONSORING / MONITORING AGENCY NAME(S) AND ADDRESS(ES)

US Army Aviation Research, Development and Engineering Command (RDECOM)
Aviation Applied Technology Directorate (AATD)
Fort Eustis VA 23604-5577

10. SPONSOR/MONITOR'S ACRONYM(S)

11. SPONSOR/MONITOR'S REPORT NUMBER(S)
RDECOM TR 10-D-106

12. DISTRIBUTION / AVAILABILITY STATEMENT

Approved for public release; distribution is unlimited.

13. SUPPLEMENTARY NOTES

UL Note: No proprietary / limited information may be included in the abstract.

14. ABSTRACT

A number of airfoils intended for VTOL/Rotorcraft applications were tested in the Penn State Low-Speed, Low-Turbulence Wind Tunnel, and the results of these tests compared with those predicted using the potential-flow/integral boundary-layer methods, PROFIL07 and XFOIL 6.94, the Euler solver/integral boundary-layer method, MSES 3.05, and the Reynolds-averaged Navier-Stokes solver, OVERFLOW 2.1ae. In addition, several cases were considered using the Navier-Stokes solver, FLUENT 12.1.2, which incorporates the Langtry-Menter turbulence model that has demonstrated some capability of capturing the transition process. In general, the drag predictions of the codes incorporating boundary-layer methods generally agreed better with the experimental results than did those of the Navier-Stokes solvers, while all of the theoretical methods generally over-predicted the maximum lift coefficient. The Langtry-Menter turbulence model shows promise in being able to model the transition process, including the development of laminar separation bubbles.

15. SUBJECT TERMS

Airfoils, rotorcraft, laminar flow, computational fluid dynamics

16. SECURITY CLASSIFICATION OF:			17. LIMITATION OF ABSTRACT	18. NUMBER OF PAGES	19a. NAME OF RESPONSIBLE PERSON
a. REPORT	b. ABSTRACT	c. THIS PAGE			Dan M. Somers
unclassified	unclassified	unclassified	UU	44	19b. TELEPHONE NUMBER *(include area code)* (814) 357-0500

Standard Form 298 (Rev. 8-98)
Prescribed by ANSI Std. Z39.18